Pontificia Universidad Católica del Perú
escuela de posgrado

Physical parameters identification for a prototype of Active Magnetic Bearing system

Author:

Carlos Antonio Perea Fabián

Advisors:

PhD. Julio Tafur Sotelo
MsC. Jesús Alan Calderón Chavarri

Lima, June 2016

Contents

List of Figures

List of Tables

Acknowledgements

Thank God for allowing me to develop in the profession that I wanted since I was little, Mechatronics Engineering.
This thesis work was made with help of:
Family, parents, siblings, thanks for your understanding and love.
PUCP and Concytec, thanks for scholarship, professors and places as classrooms, laboratories, library where develop the research and thinking to improve our country.
Mr. Calderón, thank you for your academic advise and bet for me, we must be change agent for this country.
Mr. Tafur and Mr. Barriga, thanks for your knowledge support during the master studio.
Mr. Moran, thanks for your knowledge support in control theory and diverse applications research.

Introduction

Rotating machines are capable of transmitting radial movement through a shaft, but as the shaft is longer emits transmission own small axial oscillations of the force generated by the axle and the load. Faced with this problem, that mean the need to set a bearing to serve as support axial forces and allow to adjust the motion transmission.

Thus, the complexity of movement transmission (high frequency and high loads) and the search for greater efficiency, the development of the bearings are to be fully mechanical but this produces much loses for heat by friction, then it becoming magnetic bearing but passive and produces a fail control when it try to move loads with highest frequency to rotate. Finally, active magnetic bearing system (AMBs) approach, where a feedback control is needed to provide an optimal response and minimize the error caused by the offset in a transverse plane at the point of load application. This latter is not applied yet and its needed development.

Active Magnetic bearings, however, also have some disadvantages such as its inherent instability, its non-linear nature and it being less damped than conventional bearings. This means that whenever must include a controller to stabilize the shaft, that obtaining a system following a given specification can be complicated, depending on the deemed specific application and the design itself mechanic should be taken into account to achieve accurate systems and they are so difficult to have a real modelling, that is necessary try to modelling and identifying the system at the same time.

On the other hand, there are several patents of complete sets of active magnetic bearings which are partially shared by maintaining a lot of firms own policies where they developed. Also in the domestic industry would be develop the same high energy, environmental impact on a variety of machines that transmit power from the transmission shaft.

This would impact on different processes or systems where equipment such as compressors, pumps, belts, gears, and all requiring a radial transmission power required. The better features of active magnetic bearing are appropriate for high-speed ma-

chine tool that is a growing industry in the country.
Also, places to hard reach such as space shuttles, where they used in energy storage systems, and other applications where it is important also the absence of lubrication, allowing its use in environments where conventional bearings not they could be used as biomedical applications and new reactor technologies nuclear.
In this thesis the algorithms and strategies for active magnetic bearing should be analysed, implemented and simulated in Matlab as well as experimentally tested in the real-time computation system for a prototype of active magnetic bearing.
Develop a general method and algorithm identification for active magnetic bearings prototype and get real system parameters that allow generate the equation of state of the system to control its further development.
The specific objectives in this Thesis are:
Develop a data acquisition system for the AMBs.
Analyse the mathematical model of the system from the real system.
Conduct experiments of a physical model for data collection.
Develop an identification algorithm for the parameters of the real AMBs.
Validate system developed by testing the prototype.

Chapter 1

State of the art

Will be explain everything concerning what there are in industry also by mathematical equations as general explanations concerning identifications methodologies to get parameters of AMBs.

1.1 Development and description

The rotary machine is a machine capable of transmitting radial movement through a shaft, but while the shaft is longer emits more transmission axial oscillations of the torque generated by the axle and the load. Faced with this problem you need to set a bearing to serve as support to axial forces and allow to adjust the transmission of motion. Also the mechanical bearings allow transmitting motion, but produce losses due to friction generated.[Bar]

Also called sliding bearings are formed in two parts, which is shown in Figure 1.1, one of the major cases of sliding bearings use, wear on the contact surfaces limited lifespan. The generation of the lubricant film, that separating a complete lubrication, requires an additional effort to raise the pressure, and is used only in large machines for large plain bearings. Slip resistance causes the conversion of kinetic energy into heat, which flows into the parts support bearing shell. We must distinguish between simple bearings (lubricated or grease lubricated), hydrodynamic bearings and hydrostatic bearings. Slip resistance which are dry friction, mixed friction or liquid friction.[Bar]

Faced with this problem arose the idea of producing zero friction with conventional bearings with passive magnetic bearings, that is only produced constant repulsion forces to cushion and stabilize the axial oscillations which are replaced. These passive magnetic bearings have great potential and its development is still recent, solve many problems of friction but it turning point came in use, because they can not control stability when the motor rotates at high speed and contrary to its use generates greater oscillations generated due repulsion.[Jin]

Figure 1.1: Sliding Bearing
By author:[Bar]

Therefore arose a new current for bearing system, Active magnetic bearing (AMB) systems, those have recently attracted much attention in the rotating machinery industry due to their advantages over traditional bearings such as fluid film and rolling element bearings.

The AMB control system must provide robust performance over a wide range of machine operating conditions and over the machine lifetime in order to make this technology commercially viable. An accurate plant model for AMB systems is essential for the aggressive design of control systems.[Young]

AMB uses electromagnetic force to suspend the rotor engine and have several advantages over conventional hydrostatic bearing mechanisms.[Noshad]

This system has several advantages such as: zero friction, efficient operation at extreme high speeds, so it is ideal for protecting the environment as it requires no lubrication, can operate at high temperatures, heavy loads and high humidity in the middle.[Noshad]

In this thesis, we propose three approaches to obtain accurate AMB plant models for the purpose of control design: physical modelling and system identification. The former derives a model based upon the underlying physical principles. The other uses input - output data without explicitly resorting to physical principles. The latter uses each of one combined for a better answer.

For each problem, a brief summary of the theoretical derivation and assumptions is given. Experimental results based on data collected from an AMB test facility at one prototype.

1.2 Modelling and System Identification

The most developed research goes to a conception of identification based on a pre modelling system and a subsequent identification to compare the ideal values of the model with the actual response of the system. This concept has basically 2 types of methods of identification systems called open loop and closed loop.[Noshad]

Most literature is developed in open systems Identification systems, among which are methods of prediction error (PEM), variable instrumentation methods (IVM), and methods of the output error (OE) loop. These methods can be used to identify unstable open loop systems AMBS.[Shilei]

However, these techniques can fail to find the global optimum if the search space is differentiable or not linear in its parameters.[Noshad]

Recently, other methods have attracted the attention of many researchers who are canonical variables analysis (CVA), multivariate outputs error state space (MoESP) sub space and state space system identification (N4SID). All these methods have satisfactory answers in MIMO systems, but their effectiveness in identifying open-loop unstable AMBS needs to be further investigated.[Noshad]

In recent years, techniques of artificial intelligence (AI) is a suitable development for the identification of non-linear open-loop unstable plant, one of the most robust techniques are genetic algorithms (GA).[Noshad]

One option is to identify the system to perform a pre-modelling system to meet the physical parameters, so that all models are governed under the same physical principles and have a similar resolution.

Continuously it explain the most studied physical models and their respective mathematical modelling based on its analysis.

1.3 The attractive-type magnetic bearings used in the United Technologies Research Centre (UTRC).

State-space system identification

A state-space model for discrete-time lumped systems is considered by the author [Young], the steady state-space function is given by the equation 1.1 and equation 1.2

where x_k is the state of the linear system at time k, u_k is the known input to the linear system (current in the coils of the inductor), y_k is the observed output response measured offset from the central axis in the engine, w_k is the unknown disturbance and v_k is the additive measurement noise by the sensor. w_k and v_k are assumed to be stationary, ergodic white random processes, with zero mean and covariance matrix.

$$X_{k+1} = Ax_k + Bu_k + W_k \tag{1.1}$$

$$Y_k = Cx_k + Du_k + V_k \tag{1.2}$$

$$E\left\{\begin{bmatrix} w_i \\ v_i \end{bmatrix}\begin{bmatrix} w_j \\ v_j \end{bmatrix}^T\right\} = \begin{bmatrix} Q & S \\ S^T & R \end{bmatrix}\delta_{i,j} \tag{1.3}$$

The objective of the equation 1.3 is to estimate the system matrices A, B, C, and D from input/output data sequences u_k and y_k, where δ_i, j denotes the Kronecker delta. Respectively; however, since the states are not directly observed, the system matrices are identifiable only to within an arbitrary non-singular state transformation. The input is assumed to be persistently exciting. [Young]

Physical modelling

The physics-based model of the AMB system at the UTRC. Fig. 1.2 shows the UTRC test facility with two radial magnetic bearings and one axial magnetic bearing. Each radial bearing has two active axes of control, the x and y axes, while the axial bearing has only one active axis, the z axis, which is also the spin axis of the facility. The axial dynamics are assumed to be decoupled from the radial dynamics which was proposed by authors[Young]. The radial dynamics therefore constitute a four input – four output multi-input multi-output plant with motion in the x–z and the y–z planes.

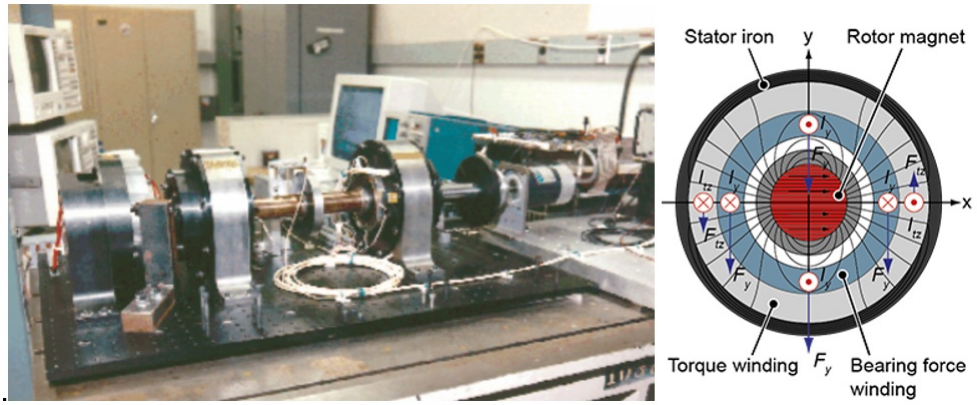

Figure 1.2: The UTRC AMB test facility
By author:[Young]

Rotor Modelling

A UTRC-proprietary rotor dynamics code was used to model the rotor dynamics

that shows in the figure 1.3. This code uses a hybrid formulation of the Finite Element Method and the Transfer Matrix method such as author says he developed by [Young] [Childs]. It can be seen that the operating speed of the facility of around 15000 rpm is above the rst bending critical of the facility.
Using the modal information generated by the above code, a linear, state-space model of the free–free rotor was developed. Details of this technique can be found in [Young] [Lee-Yoon]. The rigid body modes and the rst three bending modes are used to construct the state-space model. Modal damping is used to model the structural damping and a value of 1 % was chosen arbitrarily.
The linear state-space model obtained is gyroscopically coupled at a given running speed and is therefore parametrically dependent upon the running speed of the rotor. However, as mentioned before, a non-rotating model is used. As a result, the dynamics in the x–z and y–z.

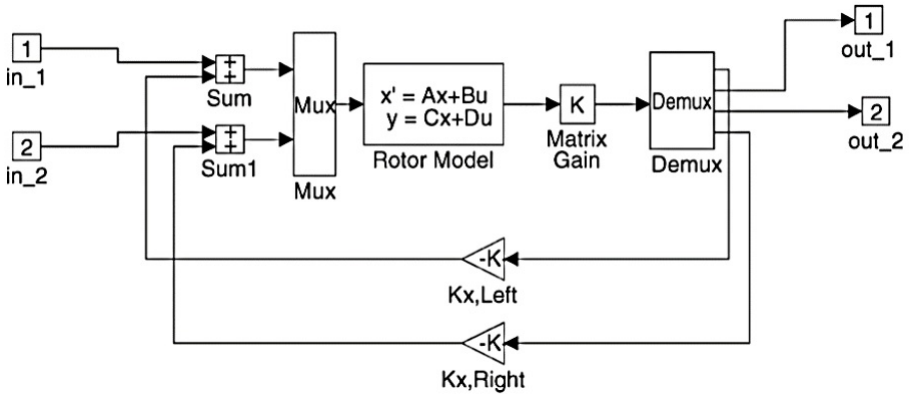

Figure 1.3: Rotor model
By author:[Young]

Magnetic Bearing Modelling

The radial magnetic bearing was designed and built at the UTRC by author [Young]. The physical equations governing the system of active magnetic bearings are described below in equation 1.4:

$$F = k_x x + k_i \frac{a}{s+a} i_c \tag{1.4}$$

where F is the force, x is the displacement of the rotor collocated with the actuator, i_c is the control current, and a is determined by the eddy current roll-off characteristics of the actuator. The coefficient k_x is called the open-loop gain of the actuator and is negative. The coefficient k_i is called the current gain and is positive. These coefficients are assumed to be constant, although they are functions of x and i_c for

large values of x and i_c. The coefficients and the eddy current pole a were determined experimentally by author [Young][Colby].

Power amplifier modelling

This model was designed and built at the UTRC by author [Young].The power amplifier is a transconductance type (voltage to current). Although this is a non linear device, it can be well approximated by a linear transfer function, given by the equation 1.5 [Young]: In which L is the inductance and R is the resistance of the magnetic bearing coil. The unknown constant K is estimated by determining the pole of the transfer function using Sine Sweep tests. This model was validated by a comparison with simulation results using non linear model.

$$\frac{I_{act}}{V_{sp}} = \frac{(K/L)}{(s + [(R + KH)/L])} \tag{1.5}$$

Sensor modelling

The displacement sensors are eddy-current-type proximity probes of KAMAN Instrument cooperation, two sensors per axis are used in a differential mode to compensate for temperature variations. These sensors are modelled using low-pass filters based on data supplied by the vendor.[Young] Using two or three sensors and applying Kalman filters can better estimate the position in the axes x and y.

Plant model

The open-loop plant model is obtained as a cascade of the sub-blocks shown in Figure 1.3. All the sub-blocks are stable except for the cascade of the actuator and the rotor model. This is shown in Figure 1.4. The open-loop gain k_x of the actuator model appears as a feedback loop around the rotor structural model and causes it to be unstable. This is analogous to a mass suspended on a negative spring.
The unstable eigenvalues correspond to the rigid body modes of the rotor. The one-plane (x or y) model will have two unstable rigid body modes.

System identification applications to AMB systems

In this section, a subspace-based state-space system identification technique is applied to the UTRC test facility to identify a black-box model based on experimental data. Issues such as input design, model order selection, and cross-validation are discussed,since the final success of a system identification technique depends heavily upon them. Various aspects of the identified model are compared with those of the

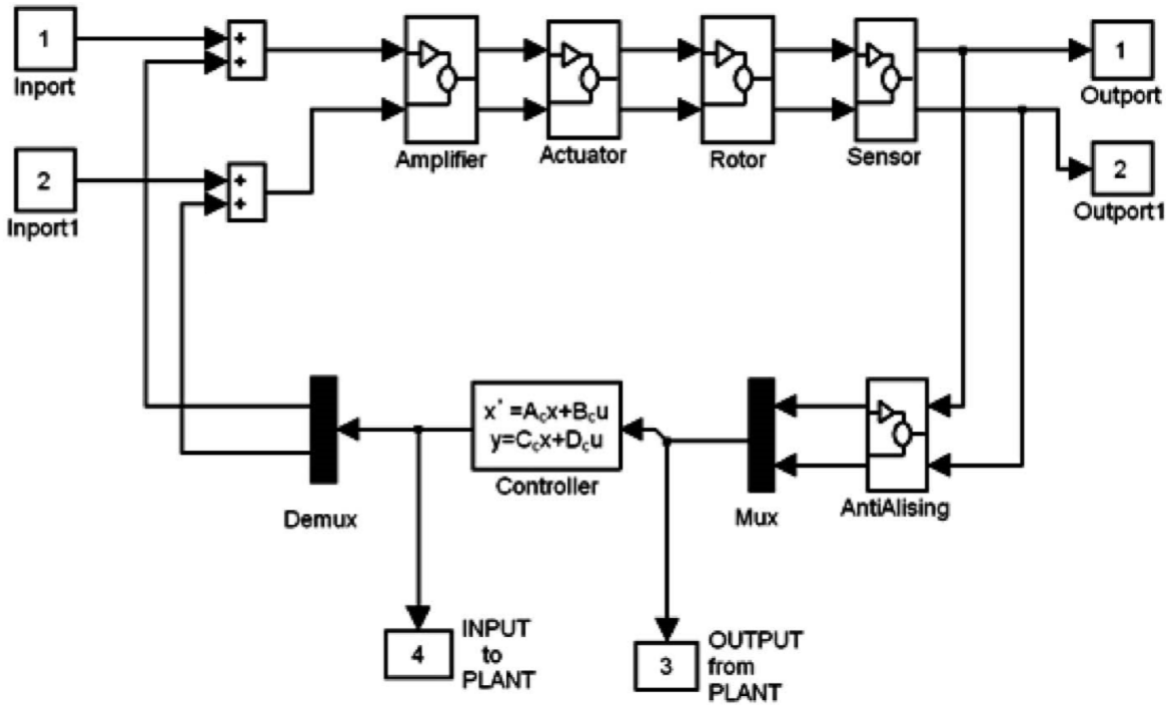

Figure 1.4: The AMBs plant model
By author:[Young]

physics-based model obtained in the previous section.

1.4 AMBs using frequency response data by RMITU.

Magnetic bearing system modelling

This model has presented an identification approach based on subspace methods with an adopted Laguerre filter network that produced a continuous time transfer function model directly from the frequency response data [Mohd]. This work is actually the first attempt to implement a subspace method in the novel application of a magnetic bearing systems. Previews based on the early simulation results show that the state-space model could identify the system successfully. The figure 1.5 shows the magnetic bearing model produced by the RMIT University.

The shaft displacements are measured at four locations. The air-gap clearance in the MB actuators is 350 um, leading to a range of [-350,350] um for these displacements. These displacements are measured by using four proximity sensors from KAMAN Instrument Cooperation, whose gains are adjusted to be 4000 V/m.
In addition, there are four pairs of coils in the two bearing actuators along the four radial directions xL, yL, xR, and yR, which are driven by four power amplifiers whose static gains are adjusted to be -0.2 A/V.

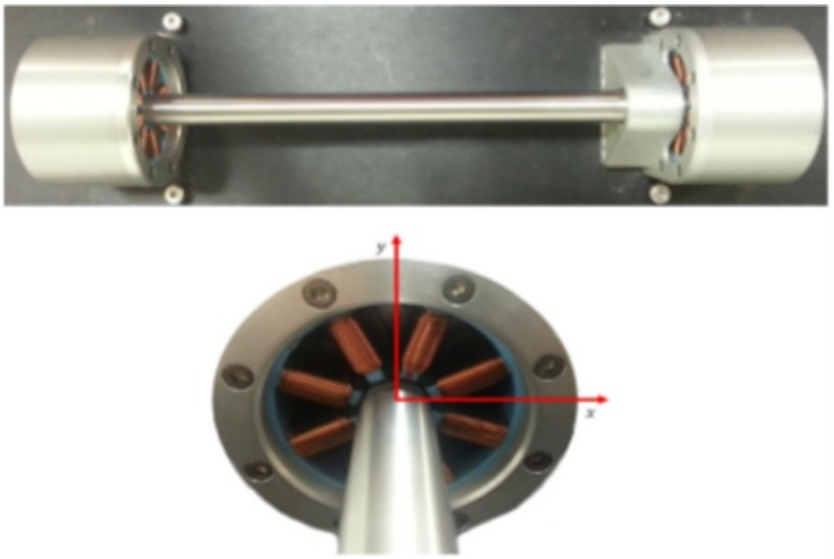

Figure 1.5: Active Magnetic Bearing model
By author:[Mohd]

The equation 1.6 by the author [Mohd] represents the force in axe x, after an approximate linearised, where the force displacement factor k_x, and force current factor k_i around the equilibrium point ($x = 0$; $i = 0$) are then calculated to be $kx = 150000$ N/m and $ki = 61$ N/A, respectively.

$$F_x = k_x x + k_i i_x \tag{1.6}$$

Another important issue in this work needing to be addressed in identification of the MB system are the rotor modes (rigid or flexible). Understanding the modes is useful in judging if an identified model is physically reasonable. A detailed discussion of the rigid and flexible modes together with other system dynamics can be found by authors [Mohd][Melbourne].

Continuous Time Subspace Identification Method Using frequency Response Data

This work examines the subspace continuous time system identification method using a network by Laguerre [Haver], in particularly with respect to the choice of the scaling factor and the number of terms.

This algorithm is applied to the magnetic bearing systems and for completeness, the subspace identification algorithm is also introduced here.

Consider the state-space models of the continuous-time system in the Laplace domain such as the equation 1.7

$$\begin{aligned} sX_{(s)} &= AX_{(s)} + BU_{(s)} \\ \mathrm{Y}_{(s)} &= CX_{(s)} + DU_{(s)} \end{aligned} \tag{1.7}$$

If the model is identified directly using $s = jw$, the identification problem becomes ill-conditioned because the condition numbers of the data matrices employed in the identification algorithm increase drastically as the system order increases. To overcome this problem, the w operator corresponds to the all-pass Laguerre filter is introduced as follows that shows in equation 1.8 by the author [Mohd].
Where parameter p>0 and it was estimated with used a mean square error (MSE) function as a guide for selection the optimal value.

$$w_{(jw)} = \frac{jw - p}{jw + p} \tag{1.8}$$

1.5 Novel Conical AMB with claw structure

A novel claw active magnetic bearing (CAMB) is proposed in this work by the author Shilei Xu [Shilei]. Compared with traditional magnetic bearings, this bearing substantially has the same radial size as the rotor diameter since its stator core and coils are both distributed in the axial space. This magnetic bearing has relatively small radial construction size, so it is suitable for use in the case when radial space is limited, such as in small machine tool spindles, submersible motors, and so on. First, this paper introduces the CAMB structure and principle, and then deduces the analytical formulas for calculating the magnetic force of this bearing using magnetic circuit method and virtual displacement principle. Finally, basic magnetic force characteristics of the designed bearing are analysed by 3D finite element method (3D FEM).

Structure and working principle

The CAMB consists of two stator components and a rotor component as show in figure 1.6, and the rotor is suspended in the air by two claw conical stators. The stator core has a structure of claw, which is composed of ring-shaped stator yoke and eight outstretched stator teeth. Each stator tooth is wound with a coil. All the eight stator teeth have conical surface on their ends. The stator core is made by ferromagnetic material DT4.

The adjacent magnetic poles have opposite polarity and their coils are connected in series, which constitute a magnetic pole pair.
Therefore, each stator is composed of four pairs of magnetic poles, which form four

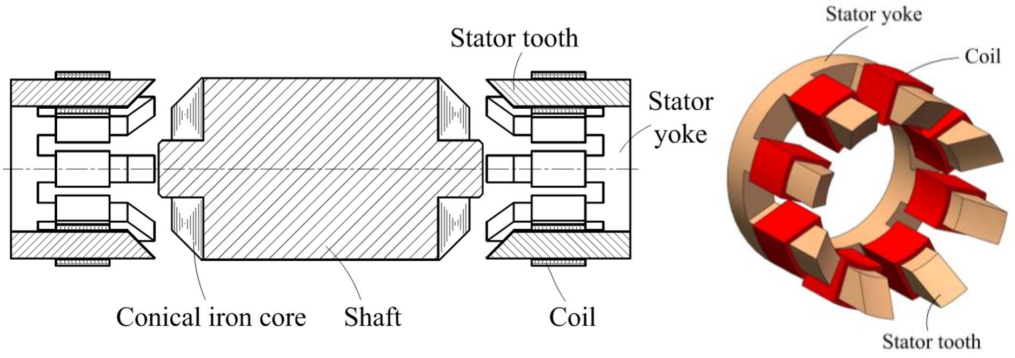

Figure 1.6: Configuration and structure of the CAMB
By author:[Shilei]

flux loops as show by the author in Fig. 1.7.

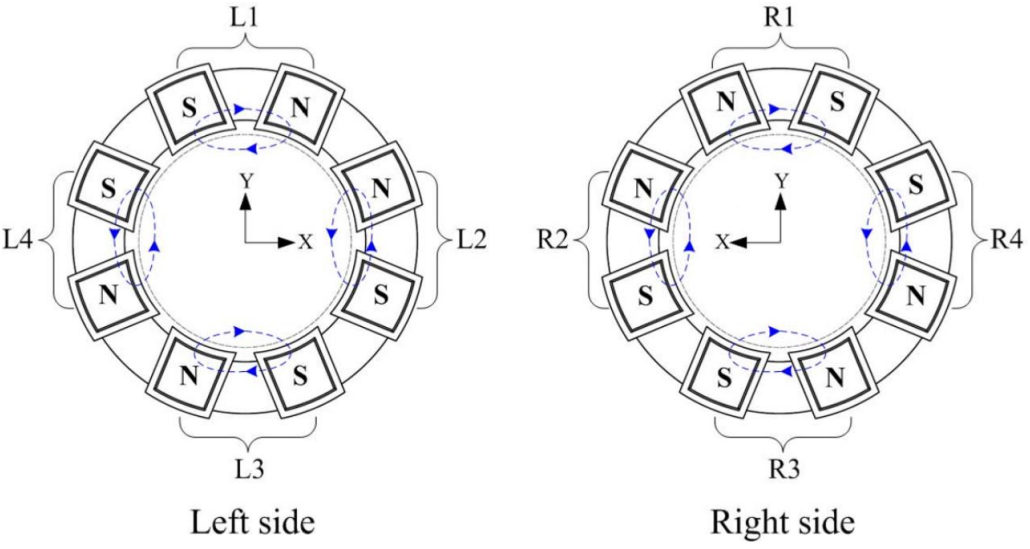

Figure 1.7: Configuration of magnetic poles
By author:[Shilei]

Analysis of magnetic force

In order to conduct the magnetic force analysis in general condition, the force of one magnetic pole pair acting on the rotor is analysed first and also takes the magnetic pole pair as show in Figure 1.8

It having a special configuration must analyse the electromotive force by equation

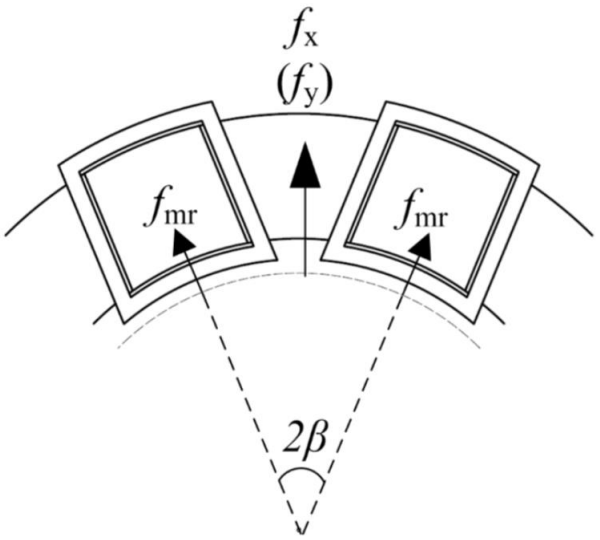

Figure 1.8: Radial magnetic force
By author:[Shilei]

1.9, where f_m is the magnetic force, u_0 is the air permeability, n the number of turns of the winding, current i, A is the area of work of each coil, and d air gap.

$$f_m = \frac{1B^2A}{2u_0} = \frac{1\mu_0\eta^2 i^2 A}{2\delta^2} = \frac{1}{2}k(\frac{i}{\delta})^2 \tag{1.9}$$

Likewise, coil current of the CAMB can be controlled by differential driving mode [Jeong], the general principle is as follows: when controlling the rotor displacement in X or Y directions, two pairs of poles in opposite position of a stator are controlled by differential driving mode, two pairs of poles L1 and L3 are controlled by differential driving mode. Similarly, L2 and L4, R1 and R3, R2 and R4 are all based on this driving mode, Figure 1.9 shows the schematic illustration of this driving mode.

1.6 Model of system Identification

The field of system identification uses statistical methods to build mathematical models of dynamical systems from measured data according to the author [Rodriguez]. System identification also includes the optimal design of experiments for efficiently generating informative data for fitting such models as well as model reduction.
All systems identification process are a sequence of steps for optimum choice. Likewise, there are various models of processes which are listed below. [Rodriguez]
Most of the systems include noise in their modelling and that describing what the difference among them is.

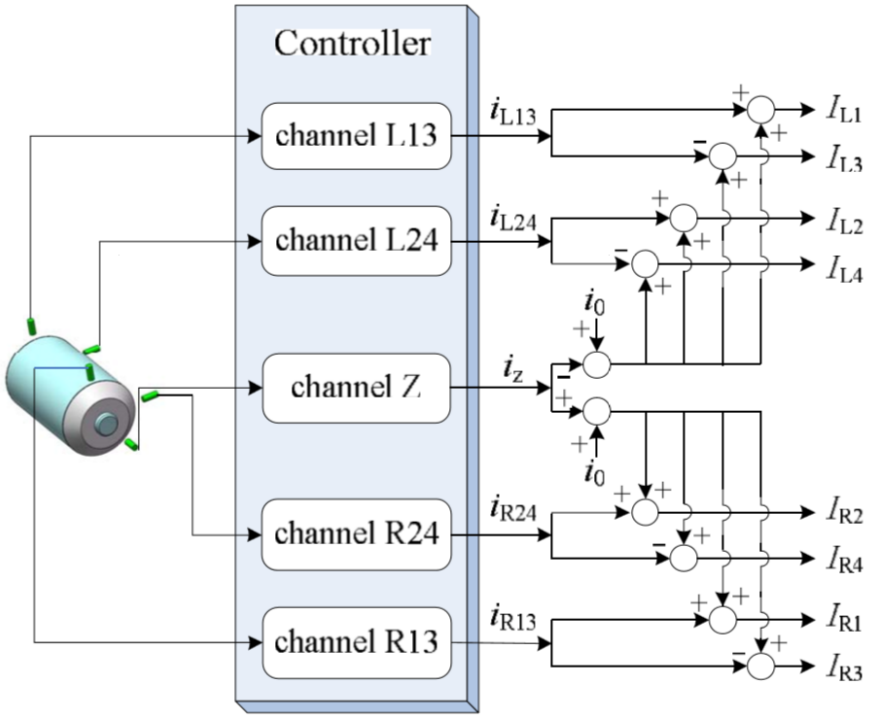

Figure 1.9: Schematic diagram of the differential driving mode
By author:[Shilei]

Box-Jenkins model identification

In time series analysis, the Box–Jenkins method applies autoregressive moving average ARMA or ARIMA models to find the best fit of a time-series model to past values of a time series as shown in figure 1.10 by the author [Rodriguez].

The notation ARMA (p, q) refers to the model with p autoregressive terms and q moving-average terms. This model contains the AR (p) and MA (q) models, this development shown in the equation 1.10.
Where ϑ and θ are the parameters of the model, ε is white noise, c a constant and X_t a series of data.

$$X_t = c + \epsilon_t + \sum_{i=1}^{p} \vartheta_i X_{t-i} + \sum_{i=1}^{q} \theta_i \varepsilon_{t-i} \tag{1.10}$$

ARMAX model

Autoregressive moving average model with exogenous inputs model (ARMAX) (p, q, b) refers to the model with p autoregressive terms, q moving average terms and b exogenous inputs terms. This model contains the AR (p) and MA (q) models and a linear combination of the last b terms of a known and external time series dt, this is more completely than Box-Jenkins as shown in equation 1.11.

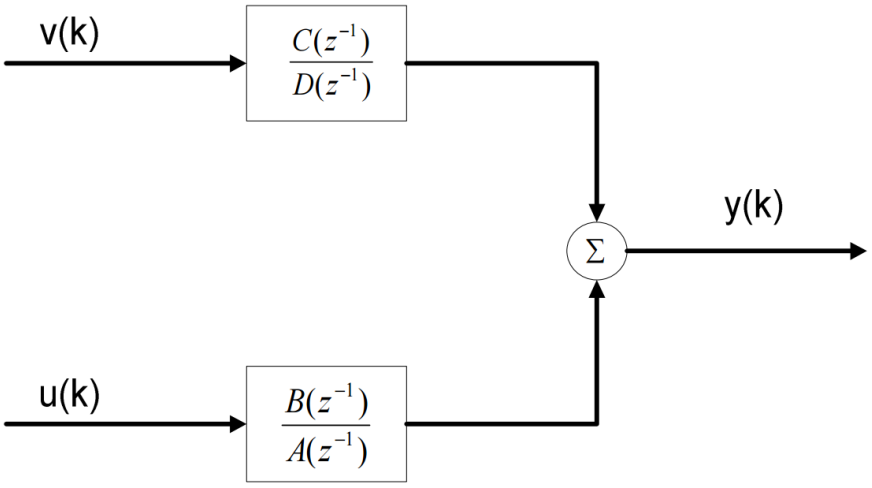

Figure 1.10: Box-Jenkins model
By author:[Rodriguez]

Where in comparison with the ARMA model, this includes $n_1, ..., n_b$ are the parameters of the exogenous input dt as shown by the author [Arafet].

$$X_t = \epsilon_t + \sum_{i=1}^{p} \vartheta_i X_{t-i} + \sum_{i=1}^{q} \theta_i \varepsilon_{t-i} + \sum_{i=0}^{b} n_i \delta_{t-i} \tag{1.11}$$

All these models are particular cases of the general structure shown in equation 1.12 evaluated by author [Arafet].
Where $e(t)$ is the filtered with noise of system, $y(t)$ output signal, $u_{(t-nk)}$ input signal, $A_{(q)} = 1 + a_1 q^{-1} + \ldots + a_{na} q^{-na}$ and $B(q) = b_1 + b_2 q^{-1} + ... + b_{nb} q^{-nb+1}$ polynomial affecting the input u, and $C(q) = 1 + c_1 q^{-1} + ... + c_{nc} q^{-nc}$, $D(q) = 1 + d_1 q^{-1} + ... + d_{nd} q^{-nd}$ polynomial affecting the white noise.

$$y(t) = \frac{B(q)}{A(q)} u(t - nk) + \frac{C(q)}{D(q)} e(t) \tag{1.12}$$

Artificial neural network identification

Artificial neural networks (ANNs) provide one method for accurate, set point-dependent system identification of the system model ad error model.
The radial basis function network (RBFN) is well-suited to system identification because the network weights are applied linearly on the output side of the network, reducing the computational requirements for real-time implementation. RBFNs use localized activation functions, thereby reducing the effects of parameter estimation in one region of the operating space (range of rotor set points) on more distant regions of that operating space. To demonstrate the benefits of intelligent system identification on robust control, two linear parameter varying (LPV) models were

identified a 2nd order system model and a 5th order error model. The RBFNs were trained using a Levenberg-Marquardt variation of back propagation of error, which try to minimize a quadratic error cost function [Gibson]. J is the error cost function and it shown in equation 1.13 by author [Gibson].

$$J = \frac{1}{2}\sum_{t}(y(t) - \hat{y}(t/w))^2 \tag{1.13}$$

Where $y(t)$ is the approximate response data and $haty(t/w)$ is the acquisition response of real data.
The network weights w to minimize a quadratic error cost function and it analysed by equation 1.14 by author [Gibson].

$$\begin{aligned} w(t) &= w(t-1) + u_t R_t^{-1}\phi(t, w(t-1))\epsilon(t, w(t-1)) \\ \epsilon(t, w) &= y(t) - \hat{y}(t/w) \\ \mathrm{R}_t &= R_{t-1} + u_t[\phi(t, w(t-1))\phi^T(t, w(t-1)) - R_{t-1}] \end{aligned} \tag{1.14}$$

1.7 System identification process

There are several types of models according to the knowledge of physic model, while more is know, the system improve own identification, so that in such cases the model gray box, which does not know all the system parameters but used estimated parameters. Also it could be classified the types of models according to parameter assignment mode and within these the most complex is optimal non parametric since you need a frequency response or infinite impulse, in the case of AMBs is recommended frequency response by type of system response.[Rajiv]
To develop a model should have the following structure that shown in Figure 1.11 according by the author [Rodriguez].

Data acquisition

Input signals should be simple to handle, amplitude has linear restricted area, try to maintain range of frequencies (the wider better), continuous exciting period, election of the sampling period, identification time (the amount of data required).
The experiments should reveal all the dynamics of the system and identification should be first developed in open loop then in closed loop.

Shaping data

Continuous component removal, then filtering of high frequency disturbances, eliminate low frequency disturbances, eliminate erroneous data, scale the variables and

Identification of delays according with the author [Rodriguez].

Choose model structure

Types of models according to their knowledge about physics such as white box (Based on laws of physics), black box (Only relevant external dynamic function), and gray box (There are constants and parameters to be estimated).
Model types according to parameter assignment mode such as parametric models, which are specified using a limited set of parameters. Or non parametric models, that can not be represented by a finite number of parameters (Frequency response, Infinite Impulse) [Rodriguez].

Set model

Non parametric identification techniques: Analysis of transient response (impulse, step), techniques of frequency (Fourier spectral analysis), analysis of correlation (Periodic signals, stochastic), techniques for processes with unknown structure, and analysis complicated.

On the other hand, parametric identification techniques: Estimation Parameters (Continuous or discrete, prediction error), algorithms Least Squares and maximum likelihood estimator, requires know the structure of the model, and uses a function of the error.Better if there is a linear relationship between the error and parameters.

Validate structure

Lately, therefore it is necessary validate a new model of replies qualitative, following a sequence: Checking data with experimental testing, statistical test, sensitivity analysis, capacity prediction model, distortion parameter and accuracy.

Finally to validate the model redesign a controller periodically based on model and must be based on rules and heuristics that is needed.[Rodriguez]

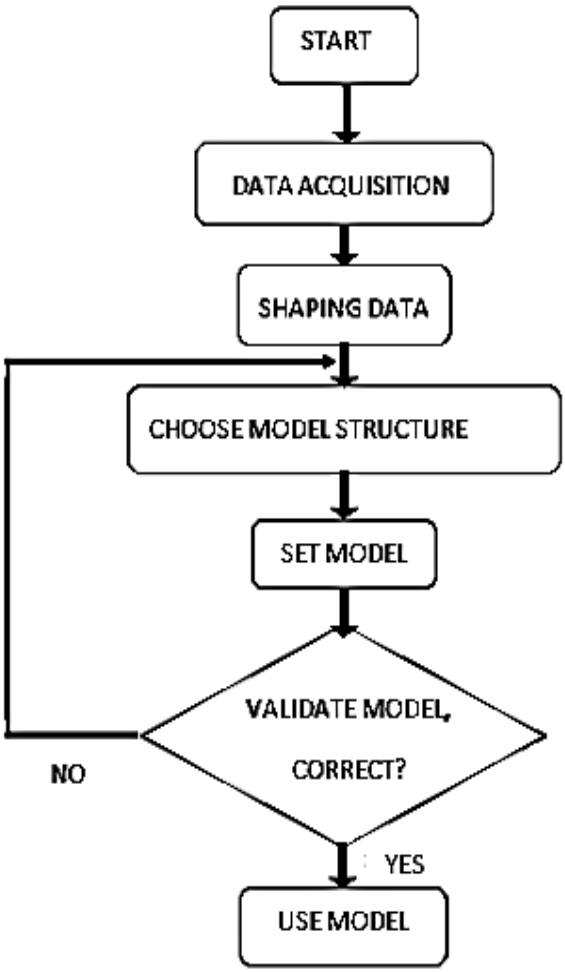

Figure 1.11: System identification process structure
By author:[Rodriguez]

Chapter 2

Active Magnetic Bearing system

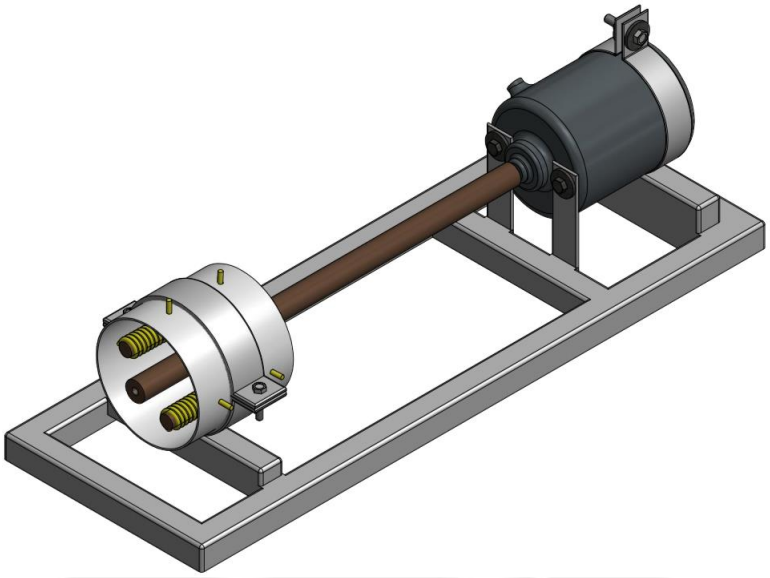

Figure 2.1: Prototype of AMB

Inside of prototypes for analyse a system of Active Magnetic Bearing (AMB), it must be consider quality of sensors, quality of mechanical and electrical equipment, therefore, in the world much institutes, universities and companies had developed different models of AMB, most importance were mentioned in chapter 1.
Likewise to develop this thesis, the thinking of prototype was developed by Alan Calderón and conditioned by own author of this thesis, the Figure 2.1 shows the prototype that will serve as a test prototype.
According to this prototype will take modelling assumptions to prove the system identifying algorithm.

2.1 Physical parameters identification

Physical parameters identification is important to combine a model of real system identification as gray box, which is able to develop a transfer function using a pre-modelling and a complex equation obtained with an algorithm of system identification.

2.1.1 Mechanical parameters

Active magnetic bearing has two most important mechanical properties which are stiffness and damping. The Figure 2.2 shown a one-axis mechanical system and its block chart of response system.

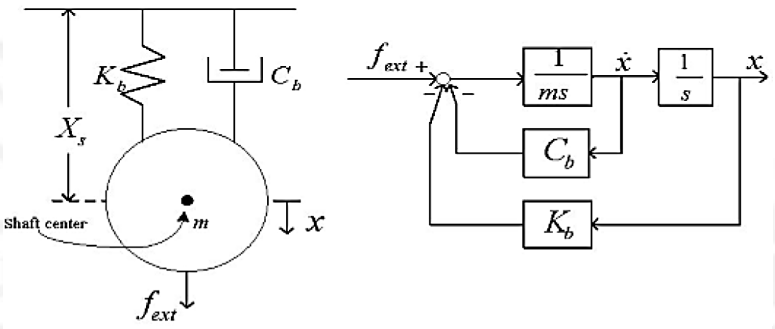

Figure 2.2: Single degree of freedom bearing model
By author:[Ki-Chang]

The motion dynamic equation of a simple mass is governed by the equation 2.1 by author [Ki-Chang]. A mass m is suspended by a spring and damper as shown in Figure 2.2. In steady-state condition, the length of the spring is $xs + x$. The spring generates a force $K_b x$, which is proportional to the spring displacement x. Also the damper generates a damping force $C_b \dot{x}$ which is proportional to the speed of displacement of x. An external force F_{ext} is also applied to the mass.
Where C_b and K_b representing the stiffness and damping coefficients of the bearing and m representing the mass of the rotor.

$$f_{ext} = m\ddot{x} + C_b\dot{x} + K_b x \tag{2.1}$$

Subsequently the transfer function that has a relation between the displacement x and external force F is shown by the equation 2.2. It is just mechanical because it

does not have influence by electrical current yet.
Where $X_{(s)}$ is the displacement occur by unbalanced load of a center reference point.

$$\frac{X_S}{F_{ext}} = \frac{1}{ms^2 + C_b s + K_b} \tag{2.2}$$

2.1.2 Electrical parameters

The system of active magnetic bearing is controlled by an external force produced for an electrical sub-system, it has a simple configuration with a resistor and an inductance load that shown in Figure 2.3

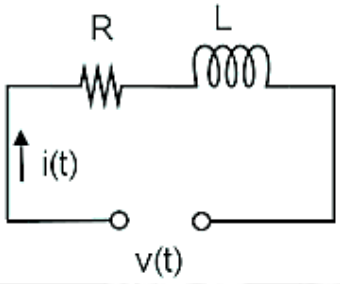

Figure 2.3: RL circuit to represent electromagnetic coil

Using laws of Kirchhoff is obtained the equation 2.3 and using Laplace transform it obtained equation 2.4 that related an electrical current with a voltage signal.

$$V = iR + L\frac{di}{dt} \tag{2.3}$$

$$\frac{I_{(S)}}{V_{(S)}} = \frac{1}{(R + Ls)} \tag{2.4}$$

First step to relate electromagnetic force with electrical current is create a magnetic force using a magnetic field, law of Ampere describes a magnetic field caused by a flow current in closed circuit. This law is shown by equation 2.5.

$$\oint H.dl = I \tag{2.5}$$

Where H is the magnetic field, is differential length and I is flow electrical current, then is possible relate with magnetic flux density with an equation 2.6. An important connection with magnetic force is using the law of Lorentz that shown in

equation 2.7.

$$B = \mu_0 H \tag{2.6}$$

$$f_m = \frac{1B^2A}{2u_0} = \frac{1\mu_0\eta^2 i^2 A}{2\delta^2} = \frac{1K}{2}(\frac{i}{\delta})^2 \tag{2.7}$$

Where $_0 = 4.10^{-7}H/m$ is permeability, H is air gap magnetic field strength, B is the magnetic flux density, n is the number of turns, A is work area and δ is the distance of air gap.

With equation 2.2, 2.4 and 2.7 is possible to obtain the electrical and mechanical parameters of the system. For electrical parameters is necessary to use an open loop control with equation 2.4 and compare the parameters with the transfer function. While it necessary to use a close loop and a preview study of behaviour the relation between electrical current and unbalance position. So the figure 2.4 shown the block diagram. Where $TF(1)_a$ is related with equation 2.4, $TF(1)_b$ is related the current produced by an unbalanced position of the rotor, and $TF(1)_c$ is related position the shaft of the rotor produced by the add between current force of unbalanced displacement and the current force of the control by electromagnetic coil.

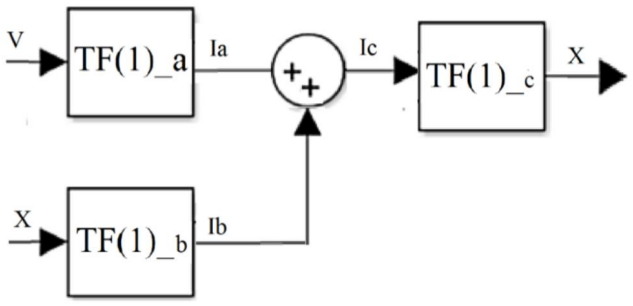

Figure 2.4: Block chart to identify parameters
By author:[Calderón]

The parameters of each transfer function is developed below with equations 2.8, 2.9, and 2.10.

$$TF(1)_a = \frac{I_a(s)}{V(s)} = \frac{1}{R + Ls} \tag{2.8}$$

$$TF(1)_b = \frac{I_b(s)}{X(s)} = \frac{K_b}{s + b} \tag{2.9}$$

$$TF(1)_c = \frac{X(s)}{I_c(s)} = \frac{K_c}{s+c} \tag{2.10}$$

Analysing the block chart it is doable to obtain the transfer function without control, thus, it is like a simple close loop control system and transfer function is shown by equation 2.11.

$$TF_{eq} = \frac{TF(1)_c TF(1)_b}{1 - TF(1)_c TF(1)_b} = \frac{\frac{K_c K_b}{(s+c)(s+b)}}{1 - \frac{K_c K_b}{(s+c)(s+b)}} = \frac{K_b K_c}{s^2 + (b+c)s + (bc - K_b K_c)} \tag{2.11}$$

Where the negative sign is because the feedback is positive and the equation solution is shown in equation 2.12

$$0 = s^2 + (b+c)s + (bc - K_b K_c) \tag{2.12}$$

By mass, spring, damping model is shown in equation 2.13.
Then by electromechanical equation is shown in equation 2.14. Using equation 2.13 and 2.14 it is possible to obtain the equation 2.15.
Where f_w is an Imbalance consideration shown in Figure 2.5, and $\hat{m}$ is the imbalance mass, e is the eccentricity of imbalance mass, θ is the angular position of imbalance mass. In equation 2.15 is not consider the force f_w cause is represented as an external perturbation of a system.

$$F = mX(s)s^2 = -CX(s)s - KX(s) \tag{2.13}$$

$$\begin{aligned} F &= k_i I(s) - k_x X(s) + f_w \\ \mathrm{f}_w &= \hat{m} e \Omega^2 cos(\Omega t + \theta) \end{aligned} \tag{2.14}$$

$$\frac{X_{(s)}}{I_{(s)}} = \frac{1}{\frac{C}{-K_i}s + \frac{K_x + K}{-K_i}} \tag{2.15}$$

Then, compare with transfer function of equation 2.10, it obtain the physical parameters of system, after to stimulate the system.
The prototype designed is a little model in which is tested control algorithms in order to achieve the control position of the rotor, by Active Magnetic Bearing. This prototype is integrated by a DC motor, a rod is fixed to its rotor, and then the rotational movement is not transmitted uniformly. Hence it is necessary to measure the changes of the rotor position that was achieved by Infra-red sensors.

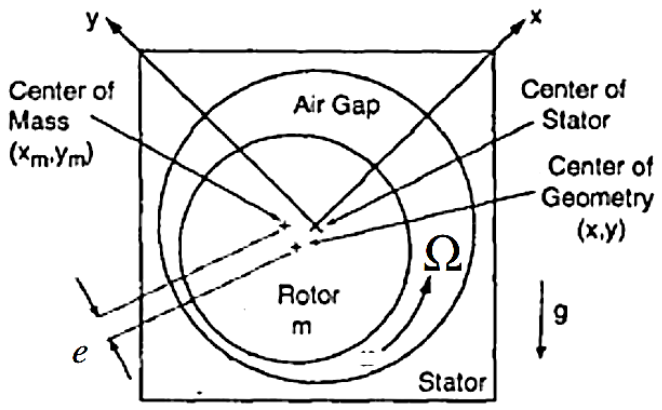

Figure 2.5: Imbalance consideration of AMBs
By author:[Guwahati]

Chapter 3

Algorithm to identify physical parameters

3.1 General system identification of AMB

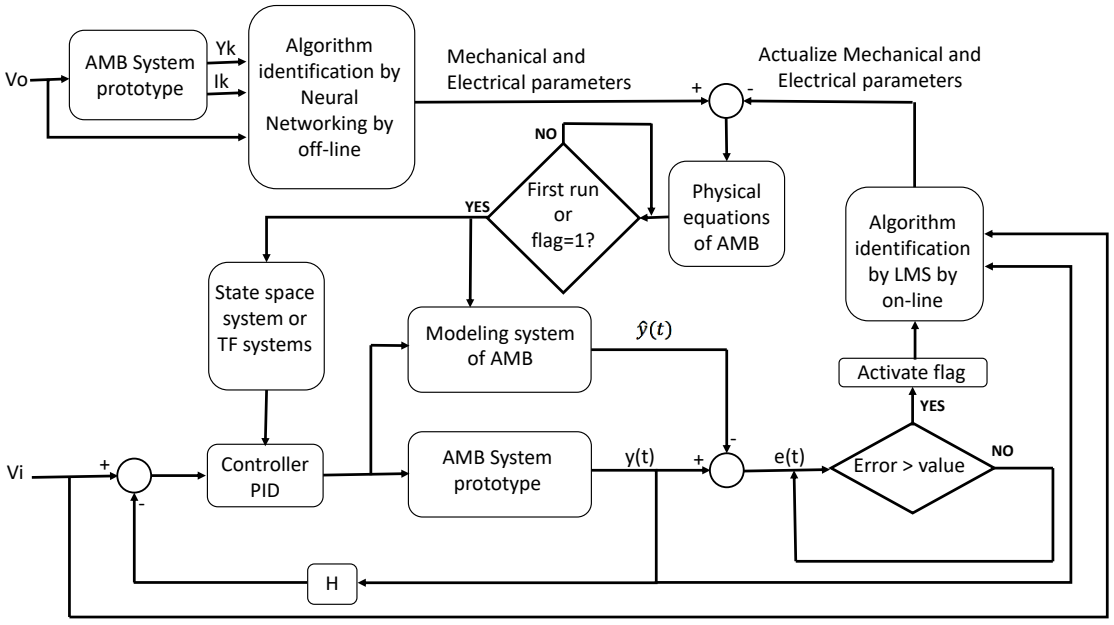

Figure 3.1: Diagram identification of AMB

After to develop different models structures to identify a system model and obtain the parameters, it choose the best performance option, a conjugation between neural networking, Narmax and LMS.

The structure shown in figure 3.1 allow obtain a good and nearly real parameters from the real system by off-line, and actualize fastly parameters when the system is run by on-line. In chapter 5 this blocks are develop inside one by one and shown the experimental results.

As a summary the AMB system run first by off-line and an algorithm based neural networking allows obtain all parameters of prototype, then when prototype is working, it could change a little these parameters because the environment and work conditions produce disturbances and electrical-mechanical parameters also change due physic conditions such as temperature, pressure, humidity, heating, etc.
In the figure 3.1 V_o represent the rich input signal to identifying the most exactly parameters, output signal Y_k position unbalance sensor and I_k current signal. Then V_i is the input signal when the prototype works and $haty(t)$ the unbalance position response of modelling system and $y(t)$ the real unbalance position, these last signal are for calculating the error system, if the error is higher than an acceptable value, actualize the system parameters. Finally the block chart H represent a proportion to communicate a signal response with a input voltage signal.

3.2 System methodologies

The model of non linear systems of differential equations is a natural representation of sampling of continuous non linear systems; provides a valid representation for a wide class of linear systems and has advantages over the series of functions.[Sedano]. From a practical standpoint, there is the need to approximate the behaviour of the inputs and outputs to simple models, affine and polynomial models are suitable output.

ARMAX

The general model is shown in equation 3.1, where F is a non linear function. The model of equation 3.2 it is known as ARMAX, for its resemblance to the linear model.
An invariant system time and non linear discrete, can be represented by the model of equation 3.1 in a region close to equilibrium point, under two sufficient conditions: That the response function of the system is finitely realizable and that a linearised model exists, if the system works chosen near the point of balance.

$$y(k) = F(y(k-1), ..., y(k-n_y), u(k-1), ..., u(k-n_u)) \tag{3.1}$$

$$y(k) = a_0 + \sum_{i=1}^{n_y} a_i y(k-i) + \sum_{i=1}^{n_u} b_i u(k-i) \tag{3.2}$$

NARMAX

Several nonlinear known models can be identified with the model NARMAX. Affine models and rational output arise in meeting the conditions of the response function of the system with respect to the polynomial function and its limit. Thus the general equations must for these models are: rational equation differences 3.3, where r

is the order of the system. And affine models, equation 3.4 with a and b are polynomials of finite degree, where a_i, with $i = 0, 1, ..., r+1$ are finite degree polynomials.

$$y(k) = \frac{b(y(k-1), ..., y(k-r), u(k-1), ..., u(k-r))}{a(y(k-1), ..., y(k-r), u(k-1), ..., u(k-r))} \tag{3.3}$$

$$y(k) = a_0 + \sum_{i=1}^{n_y} a_i y(k-i) + \sum_{i=1}^{n_u} b_i u(k-i) + \sum_{i=1}^{n_Y} \sum_{j=1}^{n_u} c_{ij} y(k-i)u(k-j) \tag{3.4}$$

Differential equations

The general equation for non linear systems can be represented as the equation 3.5. Where $G(q, \theta)$ shown in equation 3.6, $u(t)$ is input, and $H(q, \theta)$ is the polynomial of equation 3.7 varying the error $e(t)$, with $e(t)$ as a sequence of independent random variables with zero mean values. Then deriving and integrating the general equation 3.8 is obtained.

We introduce the forward shift operator q by $qu(t) = u(t+1)$ and the back ward shift operator $q^{-1}u(t) = u(t-1)$.

$$y(t) = G(q, \theta)u(t) + H(q, \theta)e(t) \tag{3.5}$$

$$G(q, \theta) = \frac{B_q}{F_q} = \frac{b_1 q^{-nk} + b_2 q^{-nk-1} + ... + b_{nb} q^{-nk-n_b+1}}{1 + f_1 q^{-1} + ... + f_{nf} q^{-n_f}} \tag{3.6}$$

$$H(q, \theta) = \frac{C_q}{D_q} = \frac{1 + c_1 q^{-1} + ... + c_{nc} q^{-n_c}}{1 + d_1 q^{-1} + ... + d_{nd} q^{-n_d}} \tag{3.7}$$

$$\int_o^T \phi_i \frac{\partial^2}{\partial t^2} u dt = \phi_i(T)u(T) - \phi_i(0)u(0) - \int_0^T u \frac{\partial^2}{\partial t^2} \phi_i dt \tag{3.8}$$

General models

All different models begin of a general family of model structures that shown in equation 3.9.

$$A(q)y(t) = \frac{B(q)}{F(q)}u(t) + \frac{C(q)}{D(q)}e(t) \tag{3.9}$$

Sometimes the dynamics from u to y contains a delay of n_k samples, so some leading coefficients of B are zero, B describes in equation 3.10, with $b_{n_k} \neq 0$.

$$B(q) = b_{n_k} q^{-n_k} + b_{n_k} + q^{-n_k-1} + ... + b_{n_k} + n_{b-1} q^{-n_k-n_b+1} = q^{-n_k} \bar{B}(q) \tag{3.10}$$

It may then be a good idea to explicit display this delay by the equation 3.11.

$$A(q)y(t) = q^{-n_k}\frac{\bar{B}(q)}{F(q)}u(t) + \frac{C(q)}{D(q)}e(t) \tag{3.11}$$

Here mostly use $n_k = 1$ and replacing $U(t)$ by $u(t - n_k + 1)$ so the predictor for 3.9.

$$\hat{y}(t|\theta) = \frac{D(q)B(q)}{C(q)F(q)}u(t) + \left[1 - \frac{D(q)A(q)}{C(q))}\right]y(t)) \tag{3.12}$$

The table 3.1 shown the different structures according the polynomials used in equation 3.12.

Polynomials Used	Name of Model Structure
B	FIR (finite impulse response)
AB	ARX
ABC	ARMAX
AC	ARMA
ABD	ARARX
ABCD	ARARMAX
BF	OE(Output error)
BFCD	BJ(Box-Jenkins)

Table 3.1: Polynomial of a model structures
By author:[Ljung]

From which we find the derivation for the coefficients show in equations 3.13, 3.14, 3.15, 3.16, 3.17.

$$\frac{\partial\hat{y}(t|\theta)}{\partial a_k} = \frac{-D(q)}{C(q)}y(t-k) \tag{3.13}$$

$$\frac{\partial\hat{y}(t|\theta)}{\partial b_k} = \frac{D(q)}{C(q)F(q)}u(t-k) \tag{3.14}$$

$$\frac{\partial\hat{y}(t|\theta)}{\partial c_k} = \frac{-D(q)B(q)}{C(q)C(q)F(q)}u(t-k) + \frac{D(q)A(q)}{C(q)C(q)}y(t-k) = \frac{1}{C(q)}\epsilon(t-k,\theta) \tag{3.15}$$

$$\frac{\partial\hat{y}(t|\theta)}{\partial d_k} = \frac{B(q)}{C(q)F(q)}u(t-k) - \frac{A(q)}{C(q)}y(t-k) \tag{3.16}$$

$$\frac{\partial\hat{y}(t|\theta)}{\partial f_k} = \frac{-D(q)B(q)}{C(q)F(q)F(q)}u(t-k) \tag{3.17}$$

Artificial Neural

Supervised learning then must find the vector of parameters , by approximating the prediction error; based on the proximity measurement, in terms of the error

criterion mean square, equation 3.18, where the vector of weights will be minimized $\theta V_N(\theta, Y)$, equation 3.19. Iterative minimization scheme is defined in equation 3.20, where $f(t)$ is the search direction and $u(t)$ is the step size.

$$V_N(\theta, Y) = \frac{1}{2N}\sum_{i=1}^{N}[y(t) - \hat{y}(t|\theta)]^T[y(t) - \hat{y}(t|\theta)] \tag{3.18}$$

$$\hat{\theta} = arg_{\theta} min V_N(\theta, Y) \tag{3.19}$$

$$\theta(t+1) = \theta(t) + u(t)f(t) \tag{3.20}$$

The error in identifying as seen in Figure 3.2 is defined as in equation 3.21. The fuzzy neural modelling discussed in this model is a type of on line Identification, then we will use the modelling error e(k) to train neural networks.
Where W are unknown weights which can not minimize dynamic modelling $u(k)$.

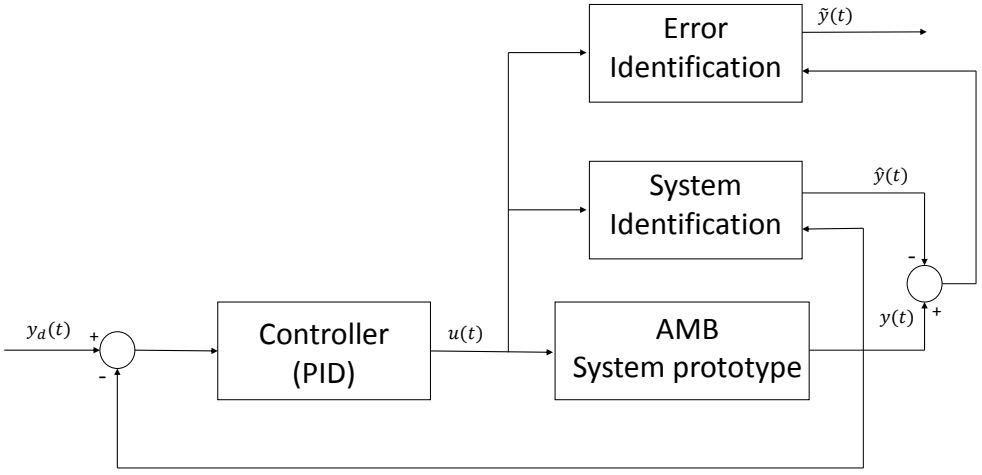

Figure 3.2: Error Identification Diagram
By author:[Heeju]

$$e(k) = (y(k) - \hat{y}(k))$$
$$\text{y(k)=x(k+1)=W}\Phi[x(k)]u(k) \tag{3.21}$$

Modelling of the non linear plant equation 3.22, the following steepest descent algorithm with a back propagation as shown in figure 3.3 with ratio of variant learning time can bounded identification error e(k). Where η is the ratio learning, and Φ is the activation function.

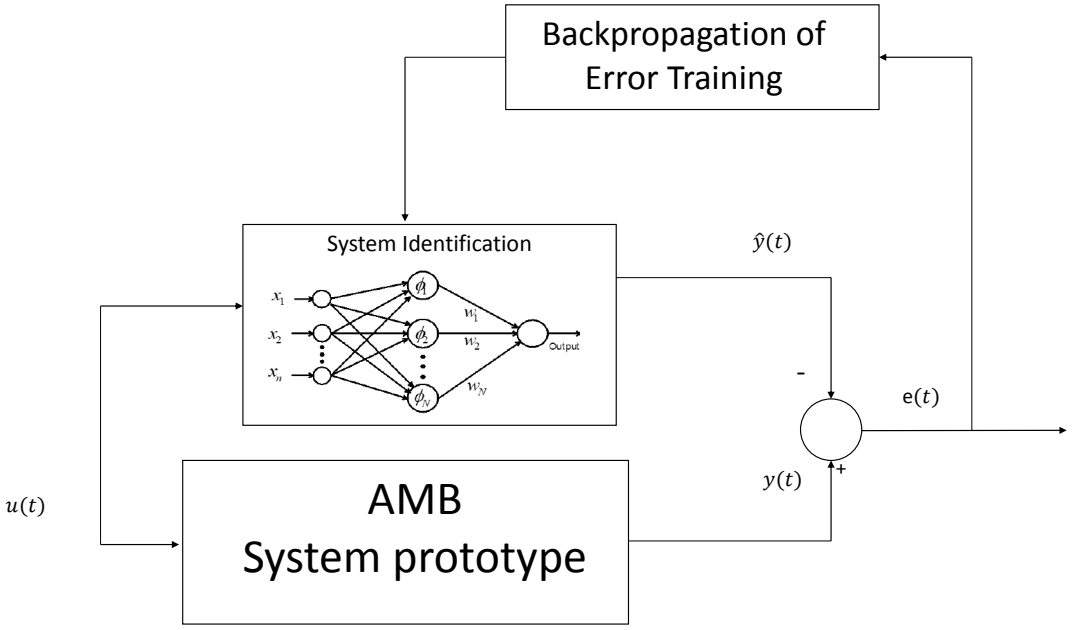

Figure 3.3: Intelligent model error identification using a non-recurrent Radial Basis Function Network (RBFN)
By author:[Heeju]

$$W(k+1) = W(k)\eta_k e(k)\Phi^T[x(k)] \tag{3.22}$$

Hybrid system (Neural Networks and NARMAX)

After making the observation $x(k+1)$, the group of regression and the network structure must be chosen; for the selection of regression, as a natural extension of the linear or non linear identification, we relied on linear models. The structures of the models will be defined by three parameters: $\Phi(t)$ vector regression, W weight vector, and $n = f(m)$ function of the neuron. Where W detailed in equation 3.22, the function of the neuron n can be Sigmoid, Gaussian, Exponential, Linear, etc.; The regression vector of $\Phi(k)$ defined below a Narmax model as shown in equation 3.23, and predictor is shown in equation 3.24.

$$\Phi(k) = [y(k-1)...y(k-n_a)u(k-n_k)...u(k-n_b-n_k+1)\varepsilon(k-1)...\varepsilon(t-n_c)]^T$$

Using recursive algorithms

$$\Phi(k) = [\Phi_1^T\varepsilon(k-1)...\varepsilon(k-n_c)]^T \tag{3.23}$$

$$\hat{y}(k|\theta) = g(\Phi_1(k),\theta) + (C(q^{-1})-1)\varepsilon(k) \tag{3.24}$$

Chapter 4

Simulation of Identifying parameters of Active Magnetic Bearing

4.1 Select an approximate model

To derive a basic AMB model, at first, any dynamics of the sensor and power amplifier electronics are neglected. In practice, this simplification leads to fairly good results if the resulting eigenvalue frequencies of the closed-loop system are not too high, i.e. if the realized bearing stiffness is in a physically reasonable range. A second simplification is that the bearing force characteristic, i.e. its dependency on coil current, rotor position and other physical quantities, is not derived in detail.[Gerhard] The mechanical stiffness of the suspension is equal to the negative derivative of the suspension force with respect to displacement: $k = df/dx$. Mathematically, the sign of the mechanical stiffness at the operating point (x_0, i_0, mg) determines the stability of this equilibrium position. For an open-loop magnetic bearing, this mechanical stiffness is negative.

The most approximate model of current of coil at off-line is determined with a simple second degree system, and its possible to obtain the resistance and inductance of the electrical part. This equation relate voltage and current as shown in equation 2.3

Solving the equation 4.1 provides a fast solution to obtain electrical parameters. Where $H = [y_k \ u_k]$, $E_{(f)}$ is the RMS error, now it minimize the error with iterative loop to obtain the least value, this is apply LMS.

$$\begin{aligned} E_{(f)} &= \sum_{k=1}^{n} (y_k - f_{u(k)})^2 = 0 \\ \Phi &= inv(H'H)H'y(t-k) \end{aligned} \tag{4.1}$$

For simulated this function its assumption transfer function is shown in equation 4.2 that is close to real parameters but random values and the result after application LMS is shown in equation 4.3.

$$\frac{A(s)}{V(s)} = \frac{550}{s + 860} \tag{4.2}$$

The figure 4.1 represent the response of the transfer function of equation 4.2, and the figure 4.2 compare between real response and system response identified.

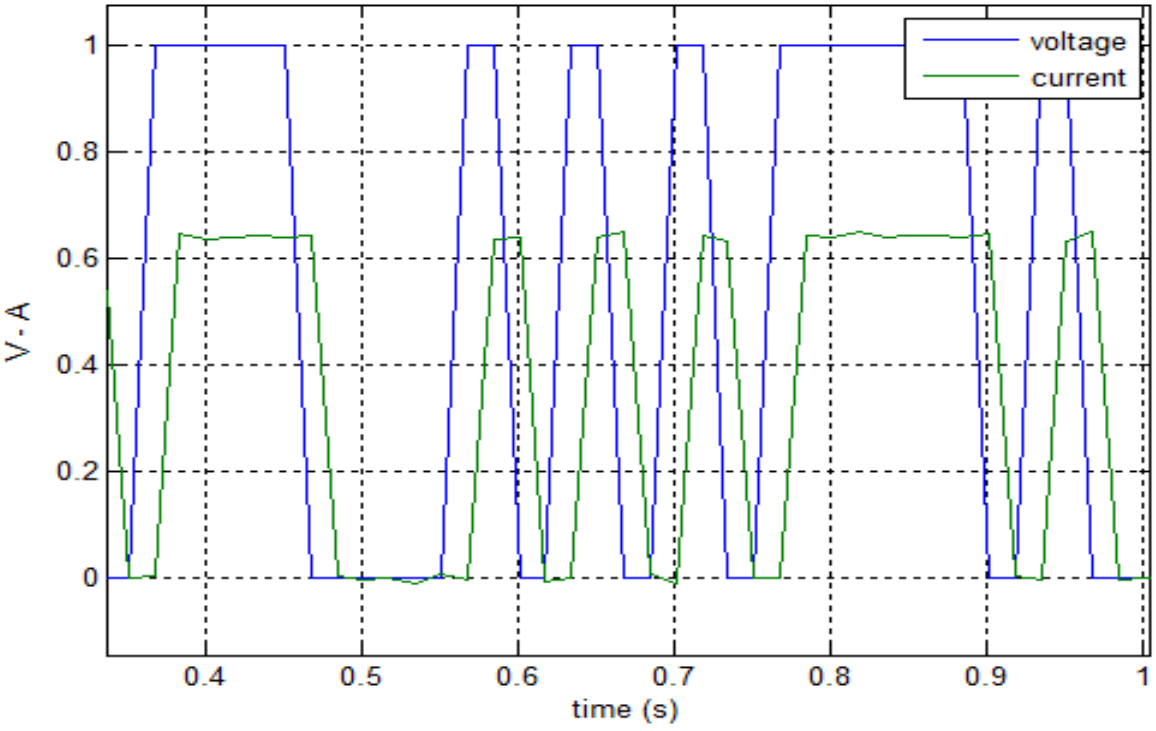

Figure 4.1: Current response of system by equation 4.2

$$\frac{A(s)}{V(s)} = \frac{519.8}{s + 812.5} \tag{4.3}$$

After identifying the electrical parameters off-line, its possible add a parameter in the equation 2.3, when it works on-line in closed loop, because as shown in figure 4.3 and 4.4, and its schematic representation shown in figure 4.5. The shaft induces a variation of current by proportional variation of position between shaft and coil.

The variation of distance S_0, induces a variation of current and the equation 2.3 becomes in equation 4.4.

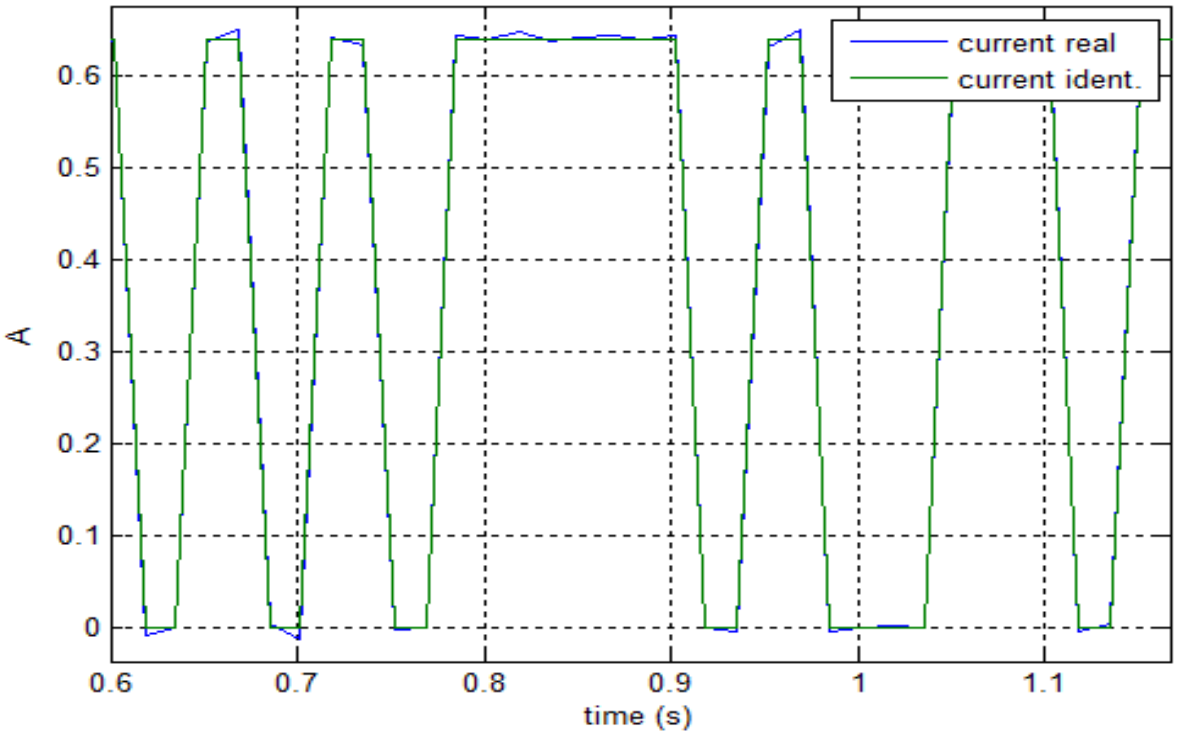

Figure 4.2: Identify current vs. Real current

$$V = iR + L\frac{d}{dt}i + k_i\frac{d}{dt}x \tag{4.4}$$

Using the equation 4.4, it obtained the variation of current represented in equation 4.5.

$$\dot{i} = \frac{-k_i}{L}\dot{x} - \frac{R}{L}i + \frac{1}{L}V \tag{4.5}$$

The same way, it solve the equation 2.14, knowing the second law of Newton says $F = m\ddot{x}$ it's possible to obtain the equation 4.6. Where m is the mass.

$$\ddot{x} = \frac{-k_x}{m}x + \frac{k_i}{m}i \tag{4.6}$$

The real behaviour of the prototype is represented as a space state system, using the equations 4.5 and 4.6, where the states are x, $\dot{x}$ and i. The state space system is represented in equation 4.7. And developed in equation 4.8.

$$\begin{aligned} \dot{x} &= Ax + Bu \\ \text{y=Cx+Du} & \end{aligned} \tag{4.7}$$

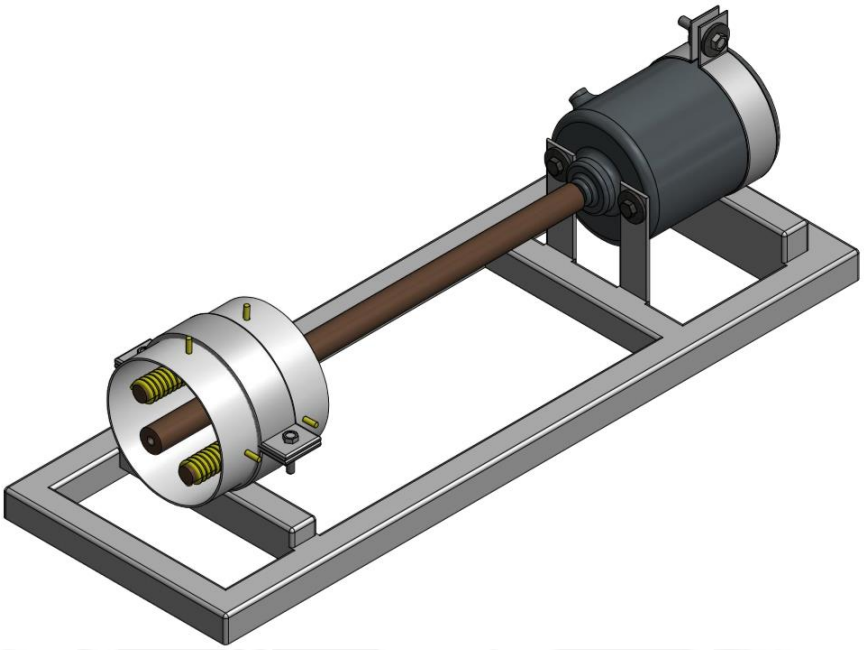

Figure 4.3: Test prototype of AMBs, isometric view

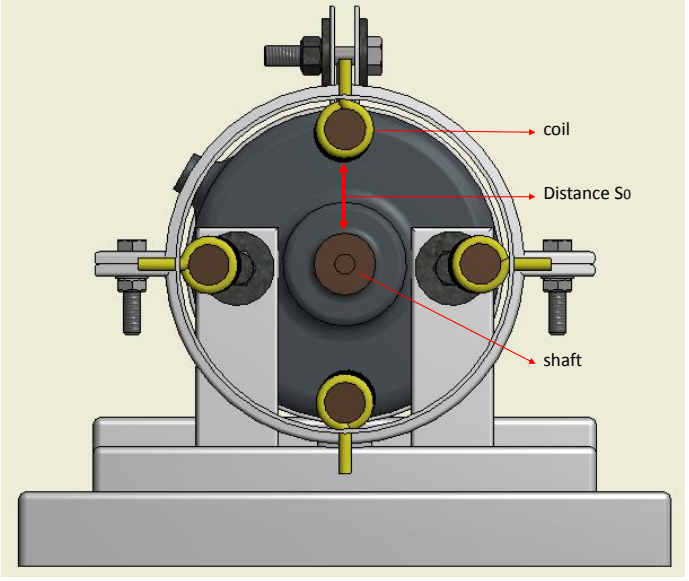

Figure 4.4: Test prototype of AMBs, front view

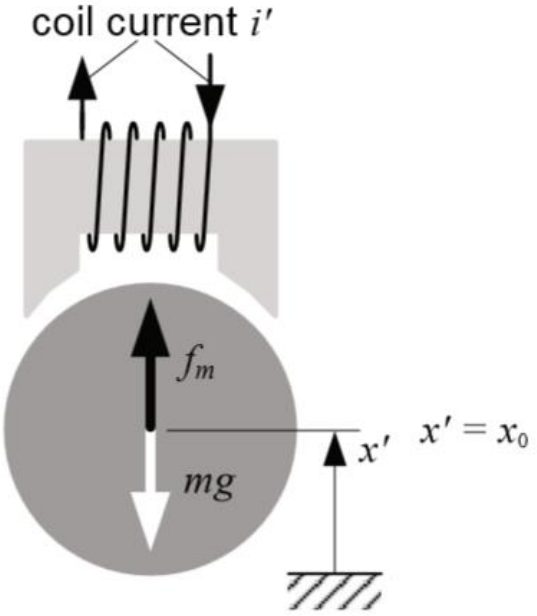

Figure 4.5: Schematic representation of AMB.

$$x = \begin{bmatrix} x \\ \dot{x} \\ i \end{bmatrix}; A = \begin{bmatrix} 0 & 1 & 0 \\ \frac{-k_x}{m} & 0 & \frac{k_i}{m} \\ 0 & \frac{-k_i}{L} & \frac{-R}{L} \end{bmatrix}; B = \begin{bmatrix} 0 \\ 0 \\ \frac{1}{L} \end{bmatrix}; u = [V]; C = \begin{bmatrix} 1 \\ 0 \\ 1 \end{bmatrix}; D = 0; \tag{4.8}$$

4.2 Identifying parameters

The real system is approximate a no-lineal system as shown in equation 4.9, but the neural network is a robust system to identify the non-linear models, it helps with a ideal model with the equation 4.7 using the parameters of the table 4.1.

$$\dot{x} = Ax + Bu + G(x, u) \tag{4.9}$$

Using the parameters of table 4.1 the matrix A and B of the system become as

Parameters	Value
mass (m)	0.1 kg
Electrical current stiffness coefficient k_i	-310.08 (N/A)
Displacement coefficient k_x	587.22 (N/m)
Resistance of coil R	1.8 ohm
Inductance L	5.96 e^{-2} mH

Table 4.1: Parameters of simulation system identification
By author:[Calderón]

values of equation 4.10.

$$A = \begin{bmatrix} 0 & 1 & 0 \\ -5872.2 & 0 & -3100.8 \\ 0 & 5202.7 & -20.97 \end{bmatrix}; B = \begin{bmatrix} 0 \\ 0 \\ 16.78 \end{bmatrix}; \tag{4.10}$$

Then after to learning by neural network it obtained the parameters of the equation 4.11. The parameters have some differences, but the total system have a good response.

$$A = \begin{bmatrix} 0 & 1 & 0 \\ -6231.1 & 0 & -3279.2 \\ 0 & 5315.7 & -18.9 \end{bmatrix}; B = \begin{bmatrix} 0 \\ 0 \\ 16.61 \end{bmatrix}; \tag{4.11}$$

The figures 4.6 and 4.7 shown the identify position and current using the ideal model by equation 4.7 to generate a state response, then add a white noise and training the system to identify the original matrix to continue with the validation.
The input signal must have a large range of frequencies and amplitudes.

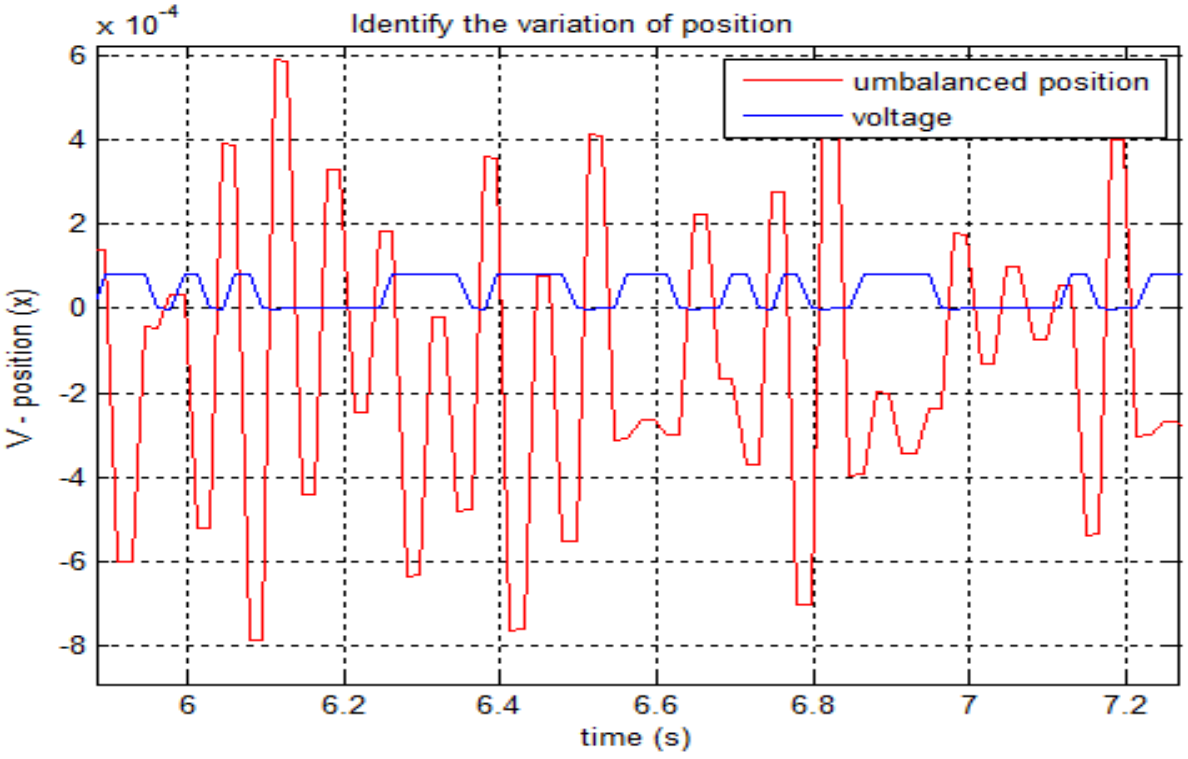

Figure 4.6: Identifying unbalance position

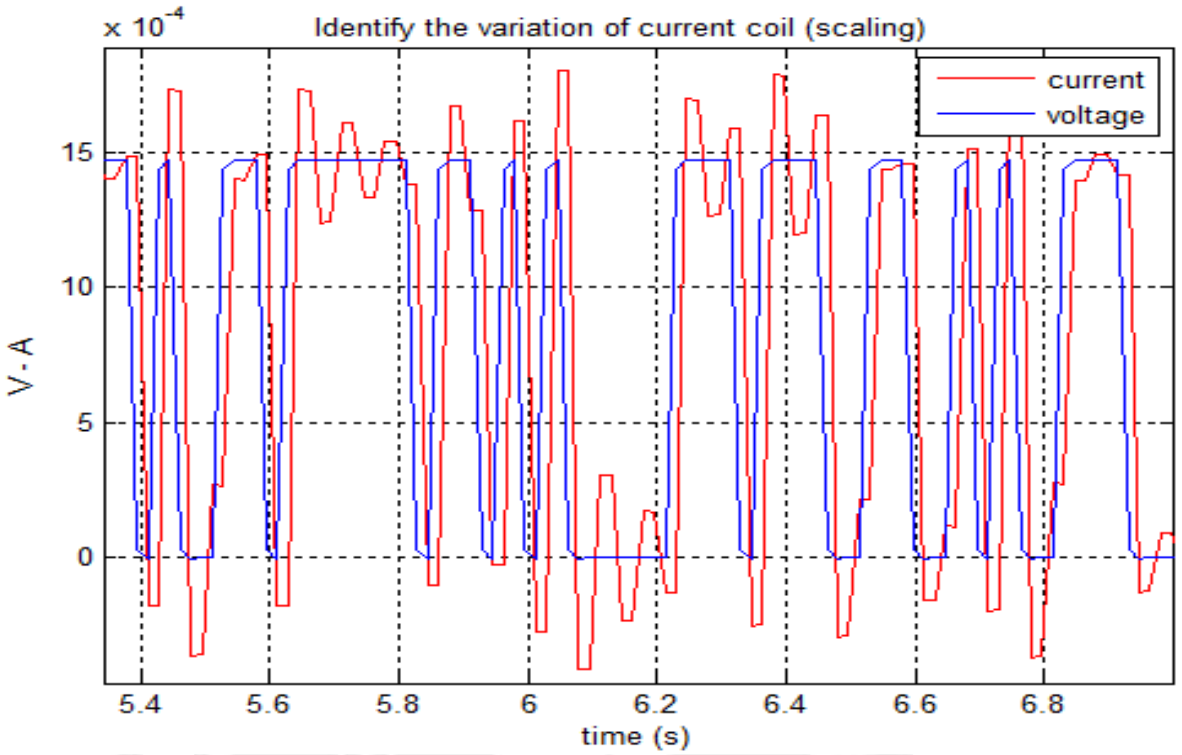

Figure 4.7: Identifying current of system

4.3 Validate model

The validation of the system is using a different kind of input signal to observe the response system.

The figure 4.8 shown the minimization error in training system, the current error descend slower than position because depends more values to identify. Figures 4.9 and 4.10 shown the validation model with a normal voltage input signal.

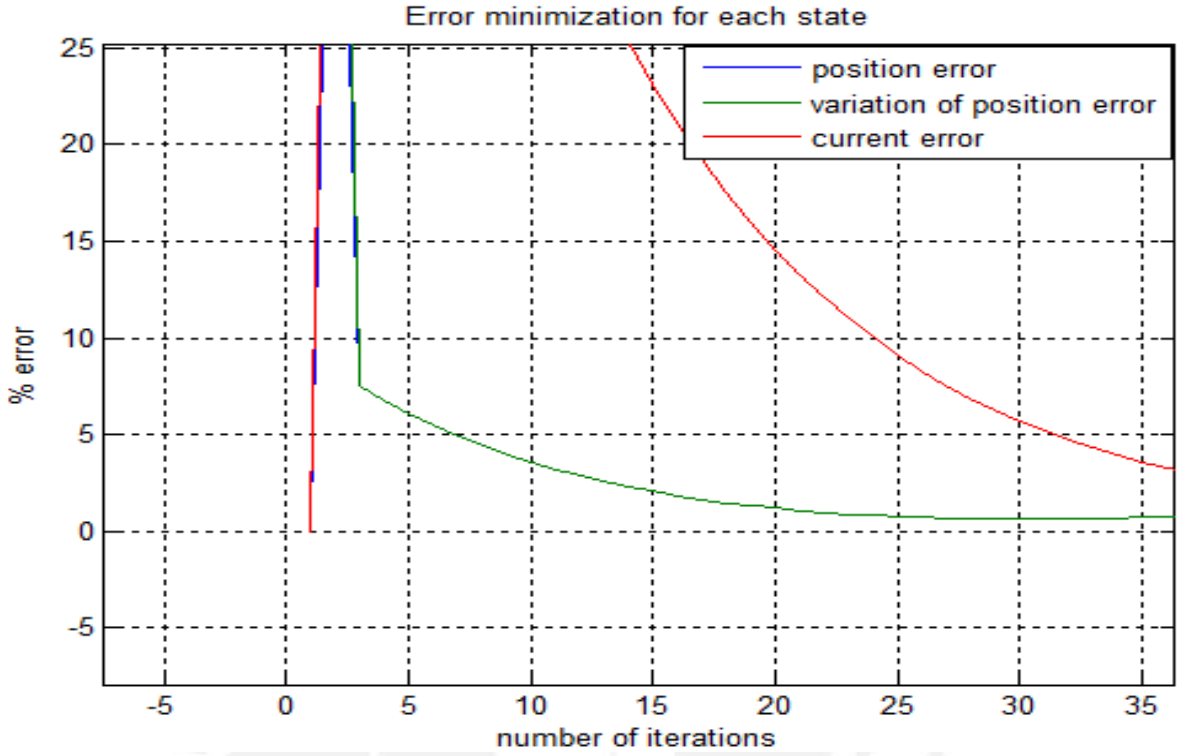

Figure 4.8: Error minimization of Ident. system by Neural network

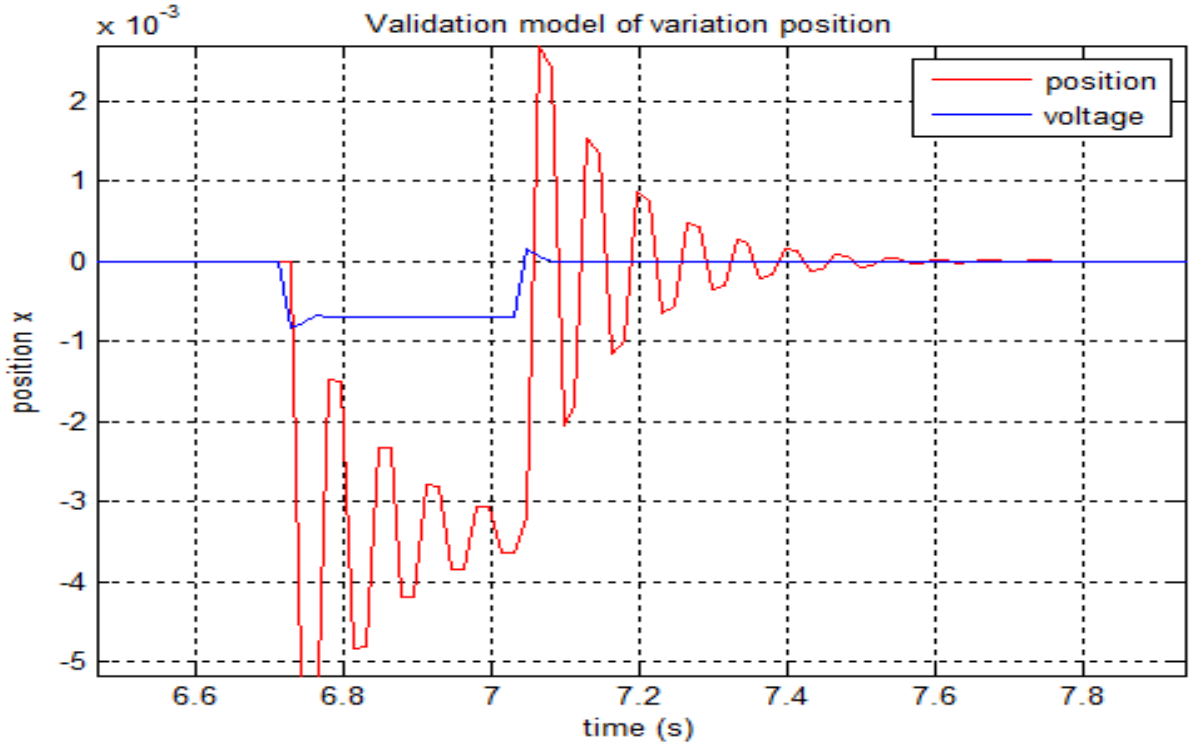

Figure 4.9: Validation model of variation position

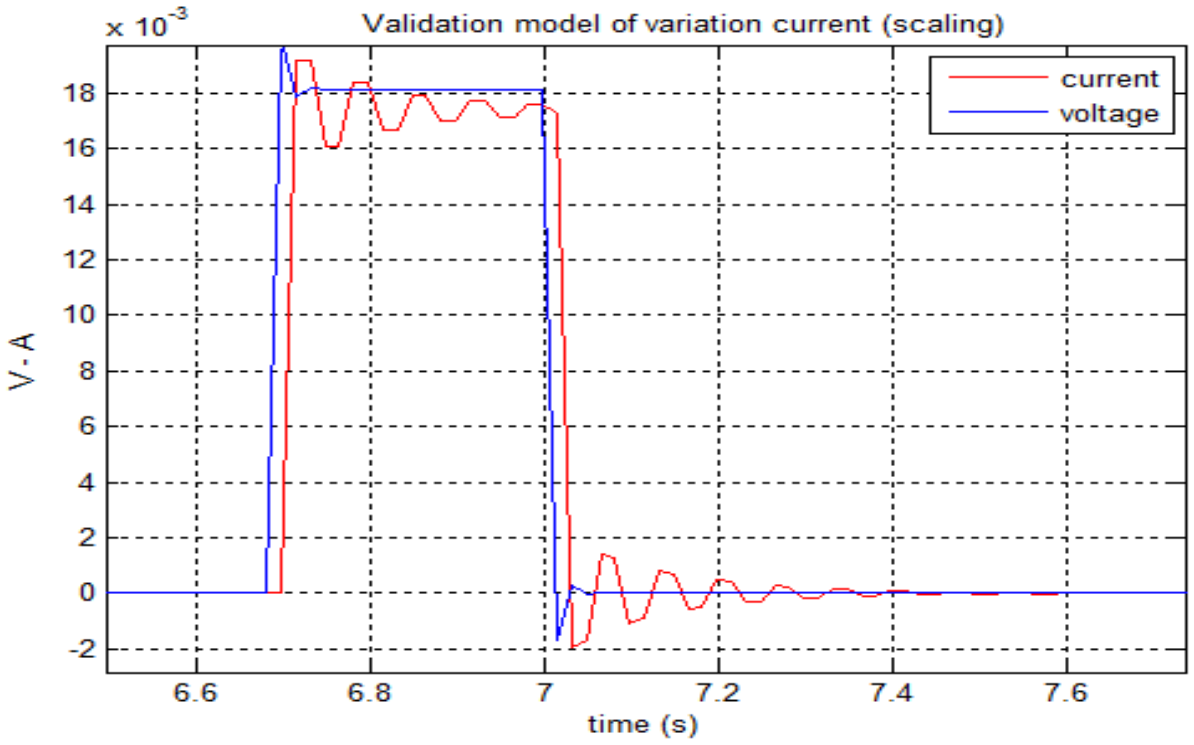

Figure 4.10: Validation model of variation current

Chapter 5

Experiments of Identifying parameters of AMBs

5.1 Mechanic prototype

Mechanic prototype of AMBs shown in figure 5.2 and 5.3 is obtained from the construction plane shown in figure 5.1. The prototype was designed by Alan Calderón, also it was improved by Carlos Perea and Danilo Aragón in order to optimize its data system identification. The first prototype shown in the figure 4.3 works with

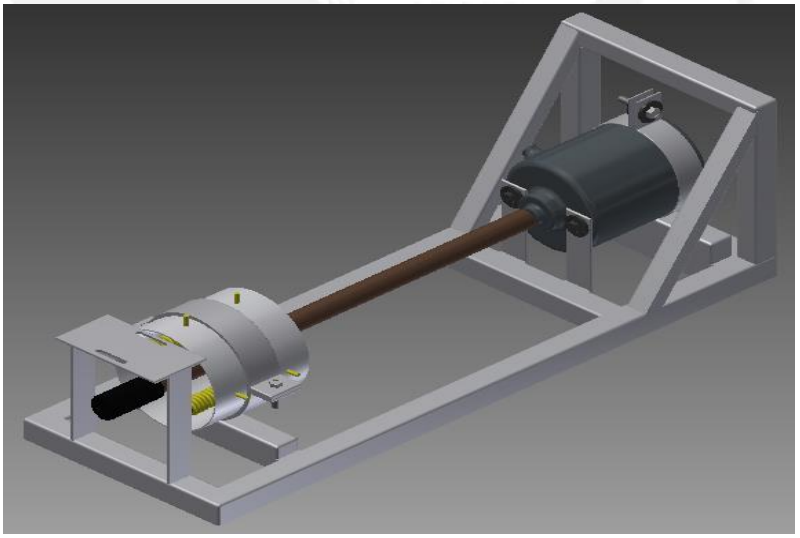

Figure 5.1: Construction plane of prototype of AMBs

horizontal shaft and it was difficult to identify imbalance position because the mass of the shaft adds a force, so the improved prototype shown in the figure 5.2 works vertical position shaft and despise the gravity force of shaft weight. In the bottom of prototype includes rubber base to damp vibrations.

The rotor shaft was not totally centered that shown in figure 5.3, but in this thesis

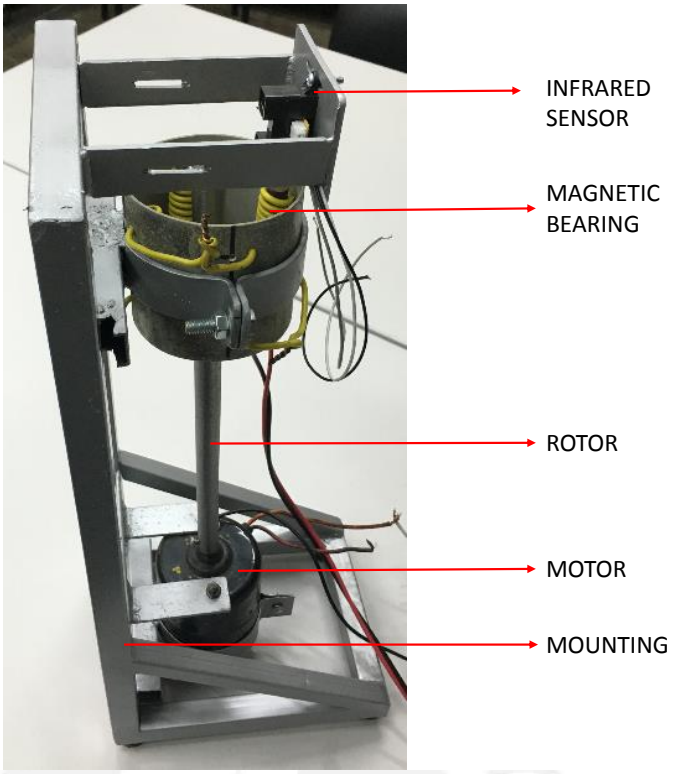

Figure 5.2: Prototype of experiment of AMBs, front view

just it identify parameters of a coil and its imbalance allow obtain better response when the coil is active.

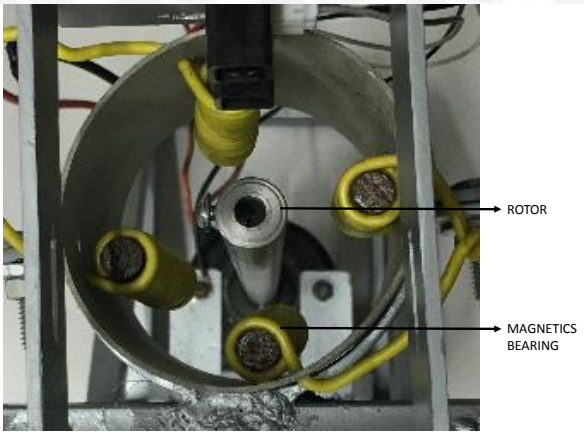

Figure 5.3: Prototype of experiment of AMBs, section view

5.2 Electronic circuits

Electronic circuit shown in figure 5.4 was designed to apply the mechanical prototype that moves a D.C. motor of 12V, so all circuits was appointed to resist more than 8A, 0.1KW and separated by potential electronic with a photodiode transistor.

The algorithm to identify physical parameters was developed in Matlab and the

micro controller is as a port between sensor, actuators with the software.

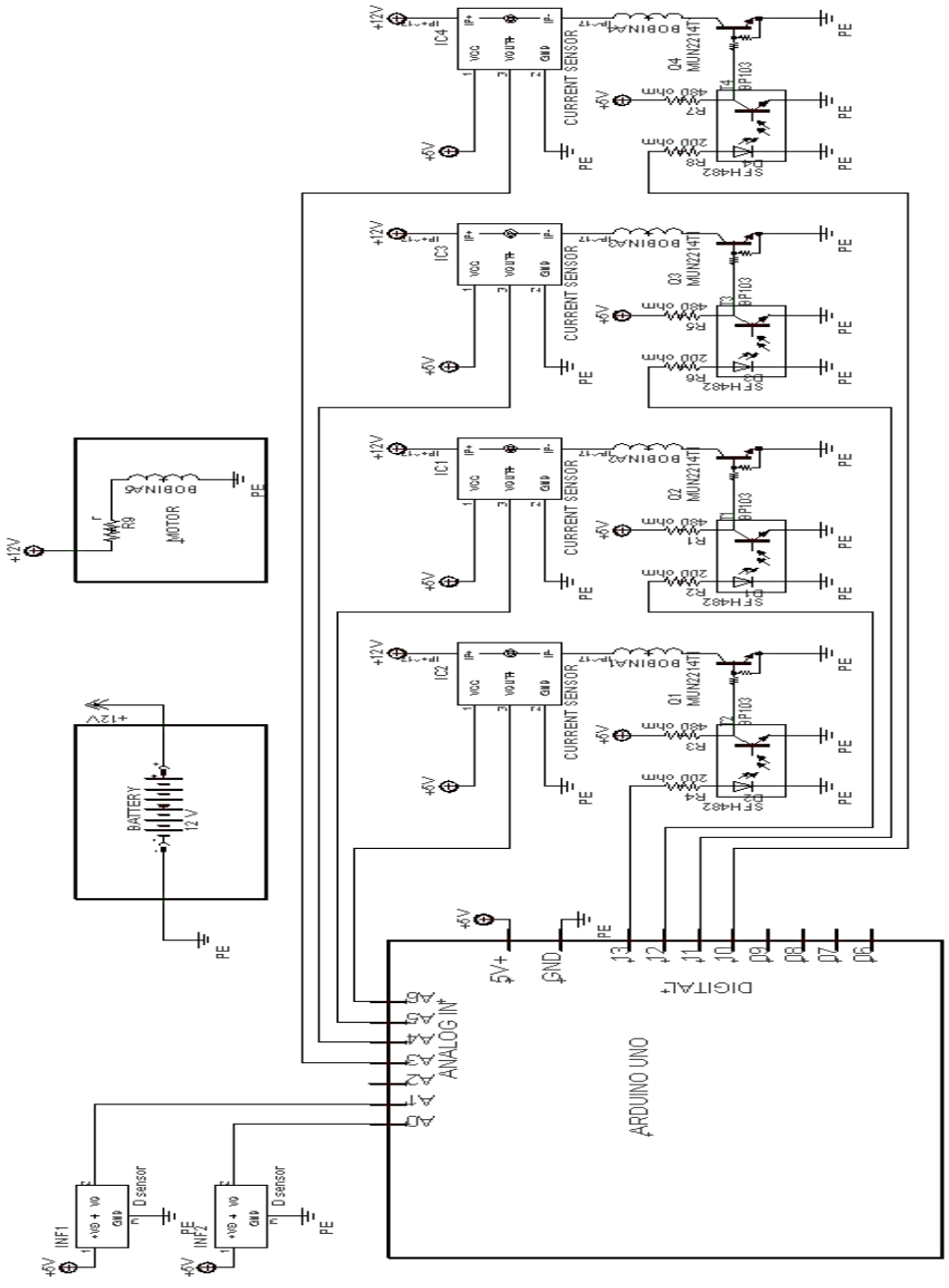

Figure 5.4: Diagram of electronic circuit

The electronic circuits include resistences, transistors and ports to a source that shown in figure 5.5. The electronic components include a source (battery of 12V), microcontroller (arduino Uno), current sensor, infrared sensor that measures the rotor shaft imbalance, shown in the figure 5.6.

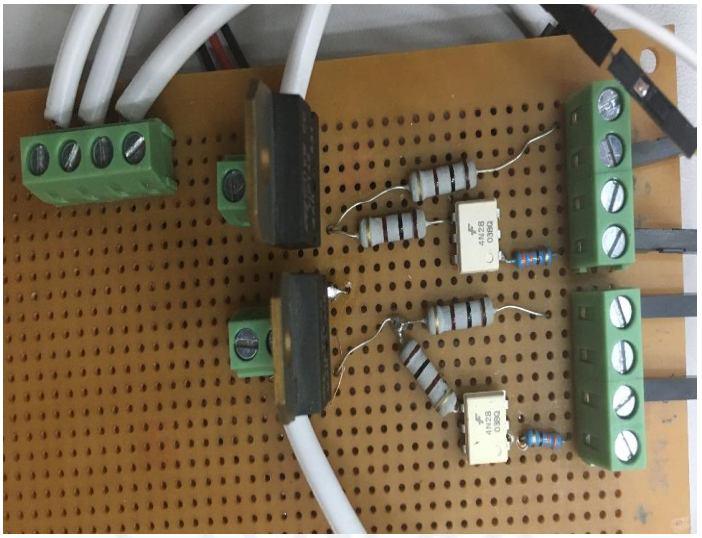

Figure 5.5: Electronic circuit

a)Arduino

b)Battery

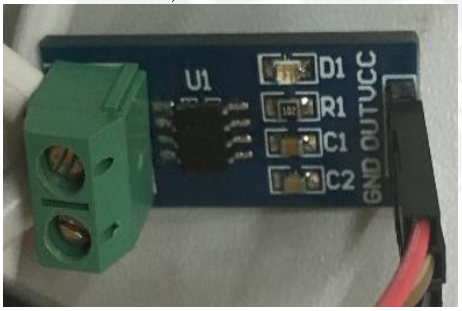

c)Current sensor

d)Infrared sensor

Figure 5.6: Electronic components

5.3 Control diagram

The control algorithm to identify parameters was designed in two parts, one to off-line by neural networking because is more exact shown in the figure 5.7 and one to on-line by LMS recursive algorithm that seems three blocks chart of first degree because is faster to run the algorithm shown in figure 5.8 and this latest is apply to

actualize the parameters.

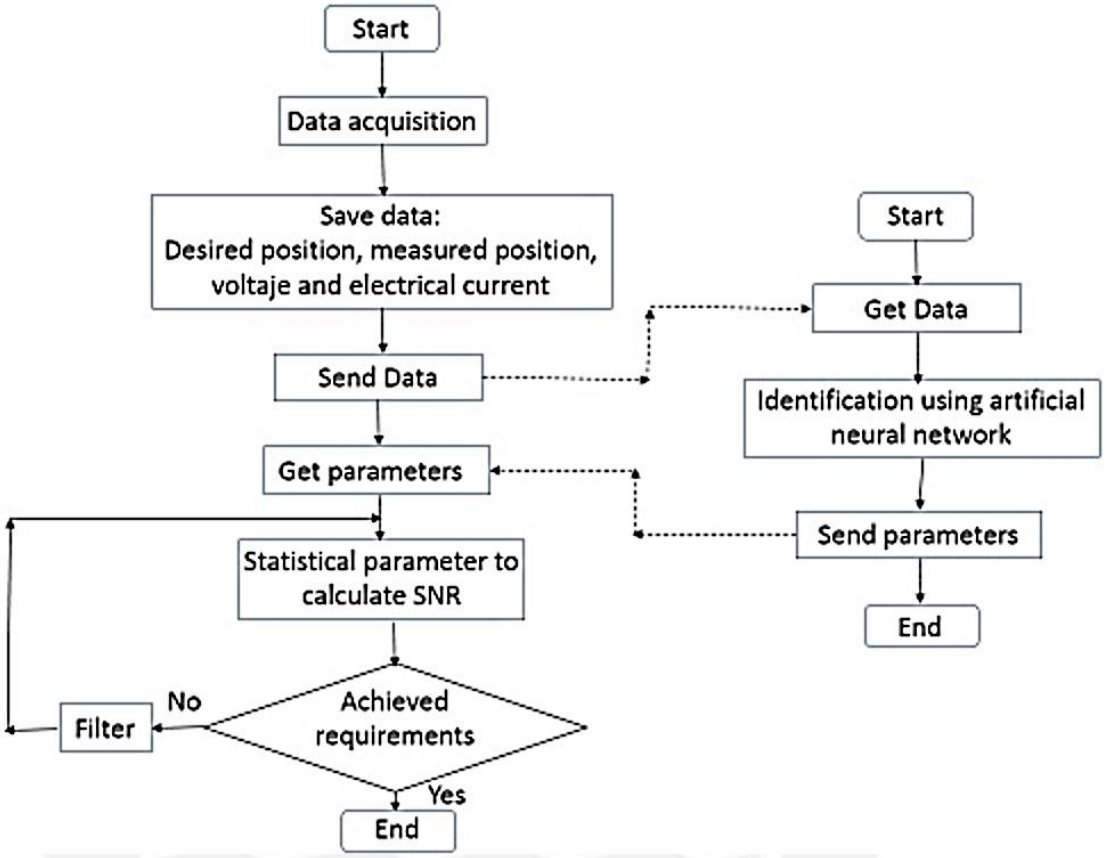

Figure 5.7: Algorithm Identification Diagram by off-line

In figure 5.7, off line controller do not need to work in few time, data acquisition is possible with a current sensor, infrared sensor to measure imbalance. Then save data such as a desired position that in this case is 20 mm, input voltage that is 12V and the values of the sensors.
After, send this parameters to a loop that allow find the matrix A and B of the state space system, using neural networking. The algorithm with neural networking is robust, so is must not include a filter after the signal of sensors.
After the parameters from Signal Noise Ratio (SNR) are calculated to evaluate if it has been satisfied user requirements, the SNR are calculated as proportion of variances $\sigma^2_{signal}/\sigma^2_{noise}$ and the noise is represented as AWGN.
Applying filter allows to get a good signal recognition, but with neural networking it enough with a good training process, so it is possible delete this requirements.

In figure 5.8, it is possible to obtain an on line controller as a result of this control strategies only if response time of the system is bigger enough than computing time.

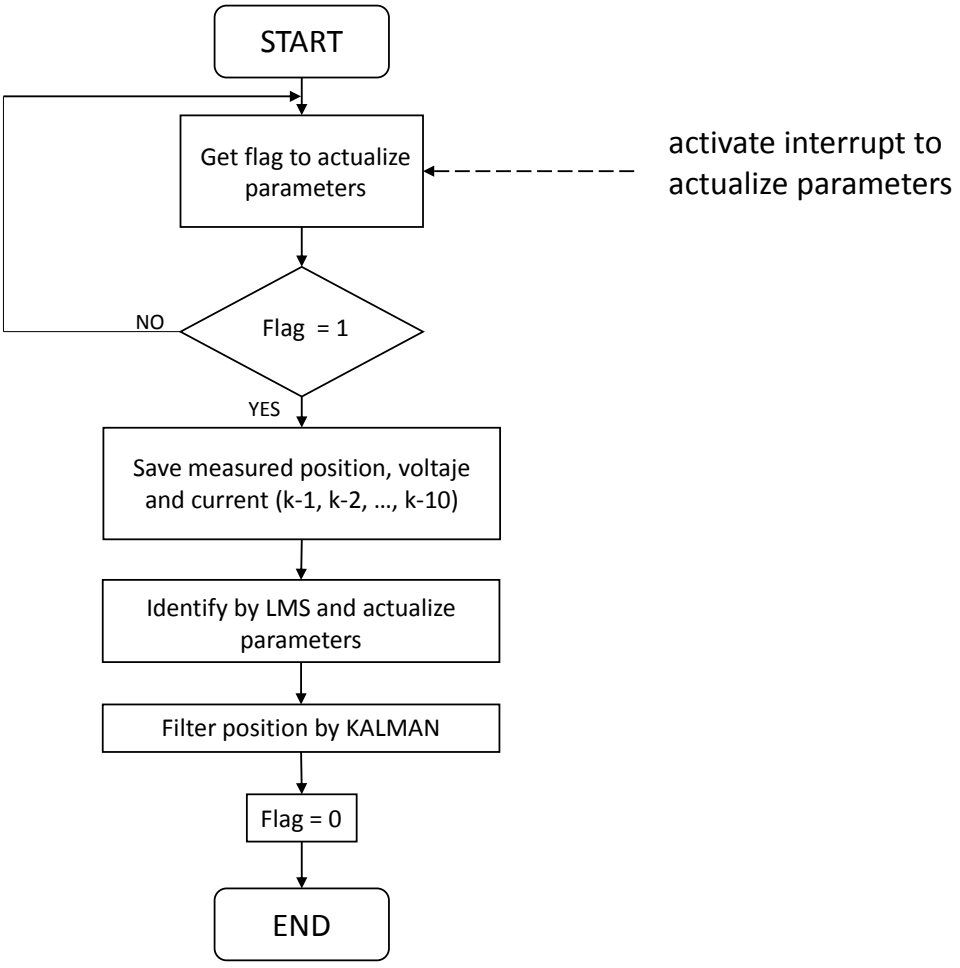

Figure 5.8: Algorithm Identification Diagram by on-line

It implies that it is possible to actualize physical parameters while control algorithm is running, also it necessary run a fast algorithm, the LMS is faster than neural networking but with a wrong response because needed a clean signal to identify, for that is applying a *Kalman* filter.

5.3.1 Neural Networking

The matrix of state space system is possible to obtain a correct shape, whether connections have same behaviour with the system, its shown in figure 5.9.
The equation 5.1 shown the relation between state space system and values of v.
According to the neural networking the equation relates the values of v with the matrix A and B with equation 4.8, and equation 5.2 shown evolution of weight v, where $J = \sum_{k=1}^{N}(y_k - \bar{y}_k)^2$, η is step size.

$$\begin{bmatrix} X_{(1)k+1} \\ X_{(2)k+1} \\ X_{(3)k+1} \end{bmatrix} = \begin{bmatrix} a_{11} & a_{21} & a_{31} \\ a_{12} & a_{22} & a_{32} \\ a_{13} & a_{23} & a_{33} \end{bmatrix} \begin{bmatrix} X_{(1)k} \\ X_{(2)k} \\ X_{(3)k} \end{bmatrix} + \begin{bmatrix} b_{11} \\ b_{12} \\ b_{13} \end{bmatrix} U_k \tag{5.1}$$

$$v = v - \eta \frac{\partial J}{\partial v} \tag{5.2}$$

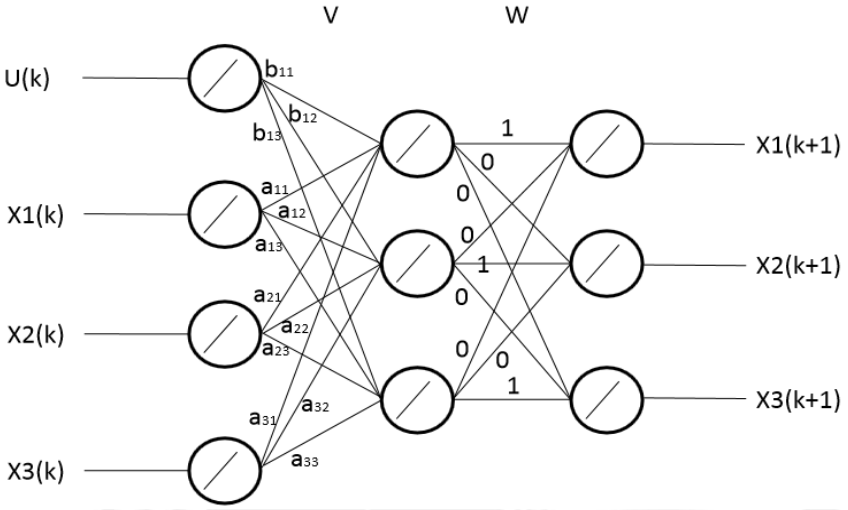

$$W = \begin{bmatrix} 1 & 0 & 0 \\ 0 & 1 & 0 \\ 0 & 0 & 1 \end{bmatrix}$$

Figure 5.9: Neural Networking modified

5.3.2 Kalman Filter

Kalman filter is an observer recursive algorithm in which the state x_k is considered using actual values. The equation 5.3 shown the state output filtered observed, where $L = SC^T R^{-1}$ and is possible obtain S with a *Riccatti* equation where $AS + SA^T - SC^T R^{-1} CS + WQC^T = 0$, $R = [\sigma n_1^2]$ (covariance of sensor), $Q = [\sigma w_1^2]$(covariance of noise), $A = [0]$, $W = [1]$, and $C = [1]$. For a good response $R = [1]$ and $Q = [60]$, this parameters was obtained trying with different values.
The figure 5.10 shown the noise obtained by the infrared sensor and how it minimize with a *Kalman* filter.

$$\dot{\hat{x}} = A\hat{x} + L(y - C\hat{x}) \tag{5.3}$$

Applying this filter in the signal measures of position it obtained the response as shown in figure 5.11.

The figure 5.12 shows the response of position filtering with a passive filter, the response is like a response with kalman filter, but in this case the kalman filter is

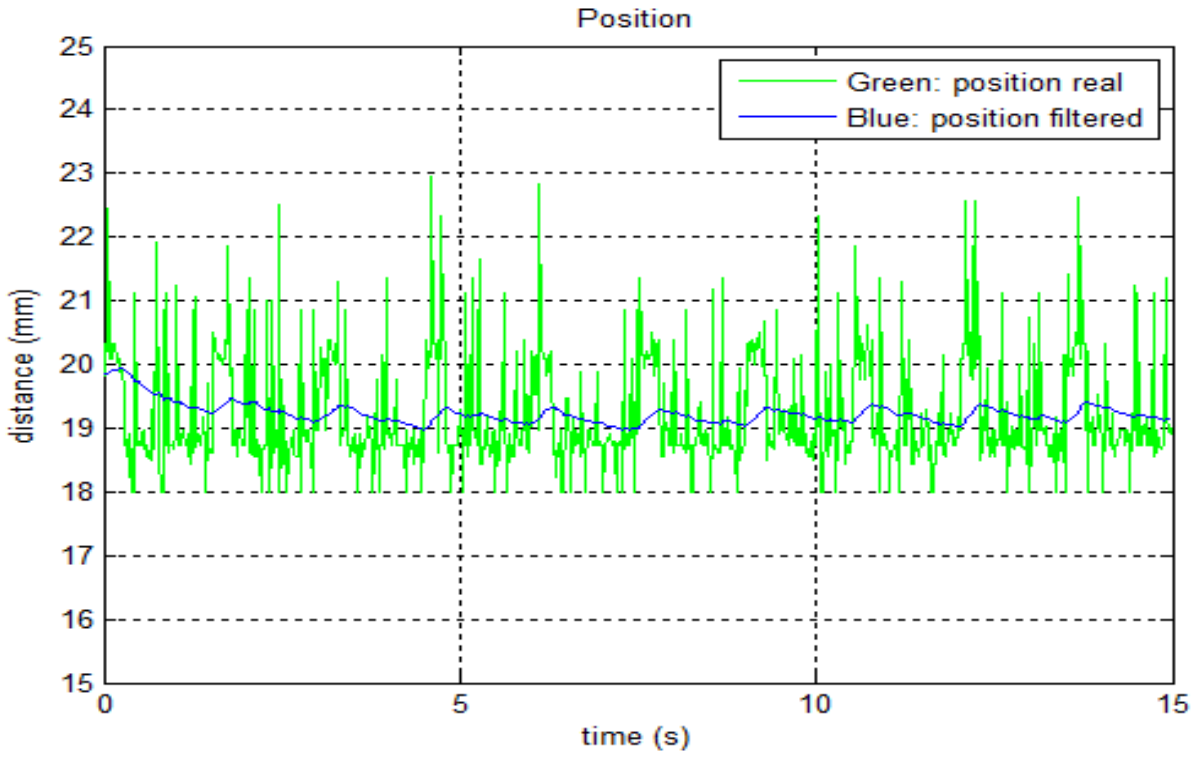

Figure 5.10: Noise filtered with Kalman filter

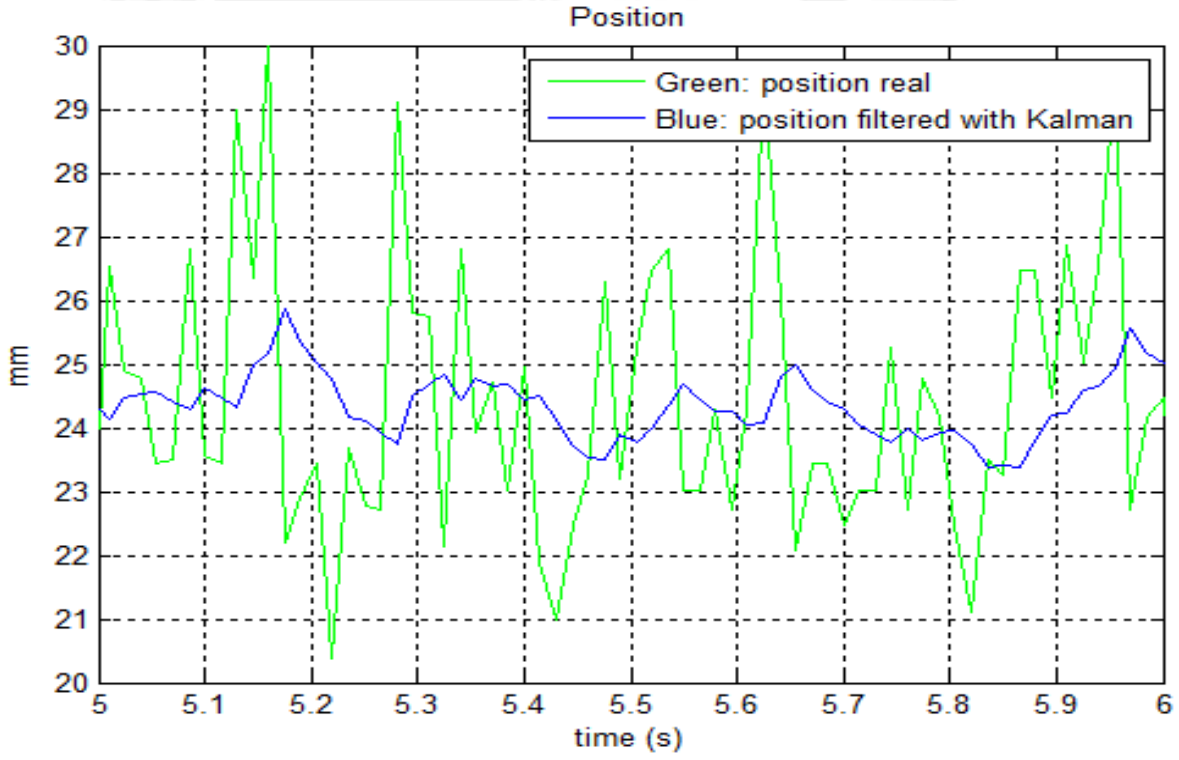

Figure 5.11: Imbalance position of shaft by kalman filter

more exact and do not consume consider computing time.

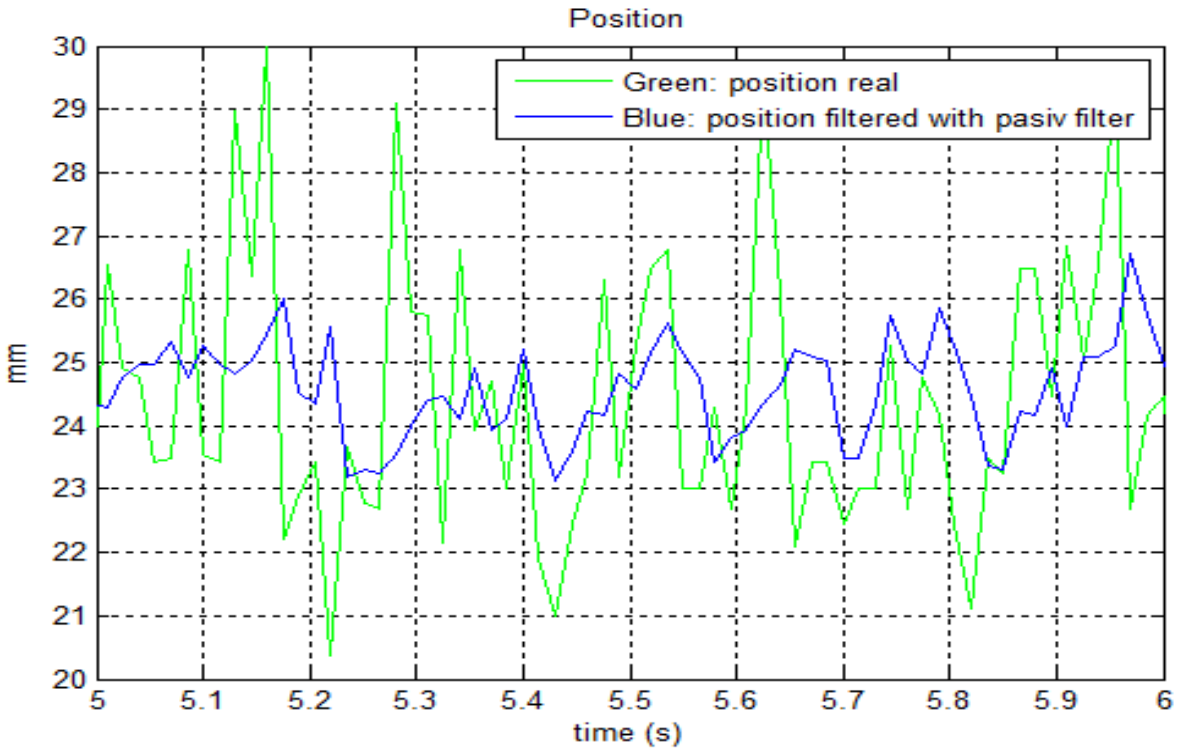

Figure 5.12: Imbalance position of shaft by pasiv filter

5.4 Identifying real system parameters

5.4.1 Identifying system with LMS

Applying the block chart that shown in figure 2.3 it is possible to find all transfer functions, all transfer functions are related with the current, after filter the position and compare with the input signal, it can observe in the figure 5.13 the action of input in the response.

The figure 5.14 shown the response electrical current with a input voltage, is not necessary apply a filter cause it measure a good response

It is possible obtain the block chart TF_{1a} with compare with a first degree system response and the equation 5.4 shown the result after identify.

$$TF_{1a} = \frac{1}{R + Ls} = \frac{653.5}{s + 1204} \tag{5.4}$$

Then the figure 5.15 shown the response of a input voltage and comparison between real current and identify current, it possible observe a delay of $0.02s$, it would be consider for a good response system identified.

Then with a output position signal is possible to obtain the transfers functions TF_{1b},

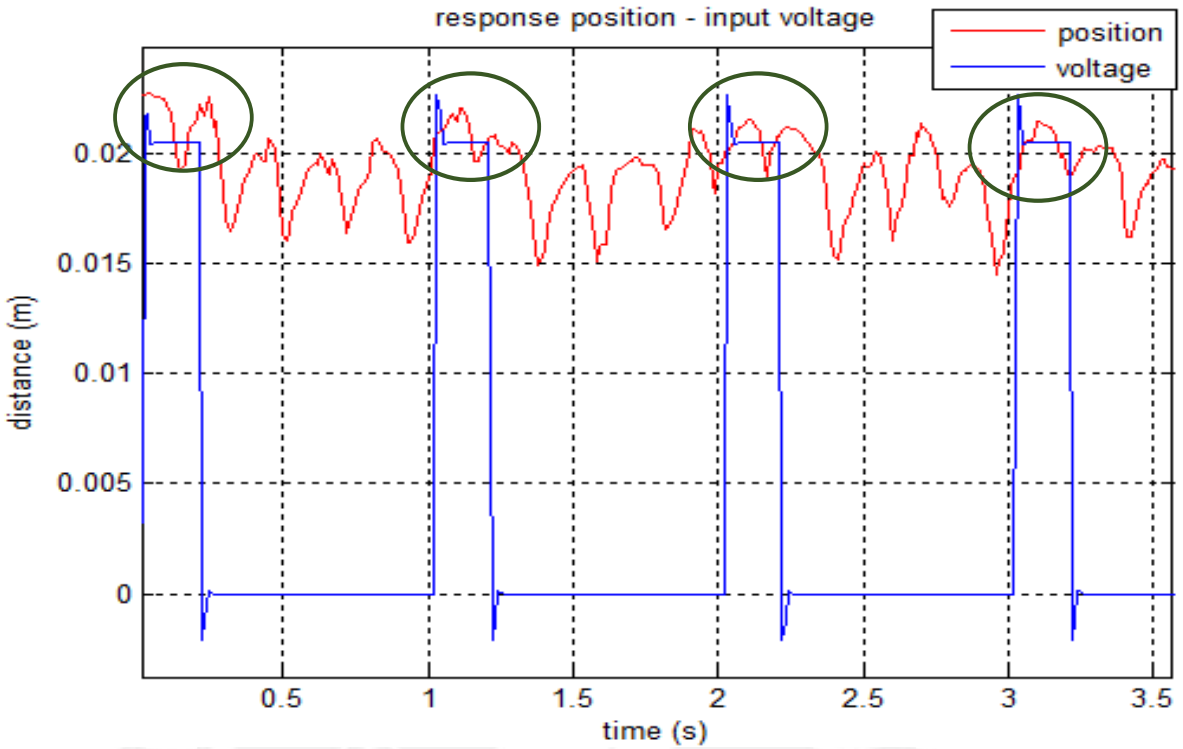

Figure 5.13: Imbalance position with a input voltage

and TF_{1c}, equations 5.5 and 5.6 shown this parameters.

$$TF_{1b} = \frac{k_b}{s+b} = \frac{0.003496}{s+1.752} \tag{5.5}$$

$$TF_{1c} = \frac{k_c}{s+c} = \frac{1.049}{s+0.07209} \tag{5.6}$$

Relating the equations $s^2 + (b+c)s + (bc - k_b k_c) = 0$ and $ms^2 + Cc + K = 0$ is possible obtain the parameters of the table 5.1.

Parameters	Value
mass (m)	1 kg
Electrical current stiffness coefficient k_i	-1.913 (N/A)
Displacement coefficient k_x	0.933 (N/m)
Resistance of coil R	1.84 ohm
Inductance L	1.5302 H

Table 5.1: Parameters of simulation system identification by LMS

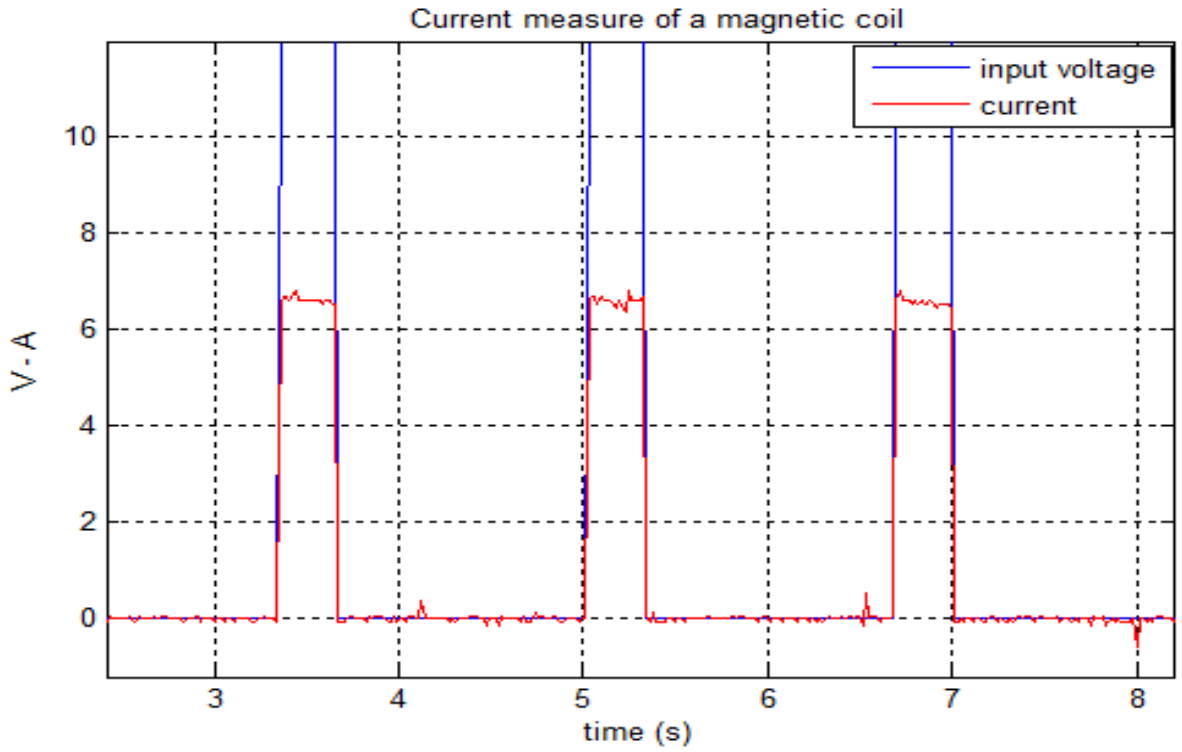

Figure 5.14: Electrical current with input voltage

5.4.2 Identifying system with neural networking

The robustness of neural networks to identify the system with added noise data. Figure 5.16 shows the values of current and voltage scaled, and the figure 5.17 shows the current identified.

The figure 5.18 shows the position estimation by neural networking.
Figure 5.19 shows minimization error response, in 10 iterations the error must stabilize and the total error minimization shown in figure 5.20 compare the time spend to identify system (0.25s approx.)
Identifying system allow obtain the matrix A and B that shown in equation 5.7, and comparison with equation 4.8 is possible obtain the parameters of table 5.2.

$$A = \begin{bmatrix} 0 & 1 & 0 \\ 0.562 & 0 & -0.603 \\ 0 & 0.0708 & -0.0371 \end{bmatrix}; B = \begin{bmatrix} 0 \\ 0 \\ 0.631 \end{bmatrix}; \tag{5.7}$$

5.5 Validate real system

Validation system is necessary to test the system identification with a rich values of input data, different frequencies.
The figure 5.21 shows the validation current estimated.

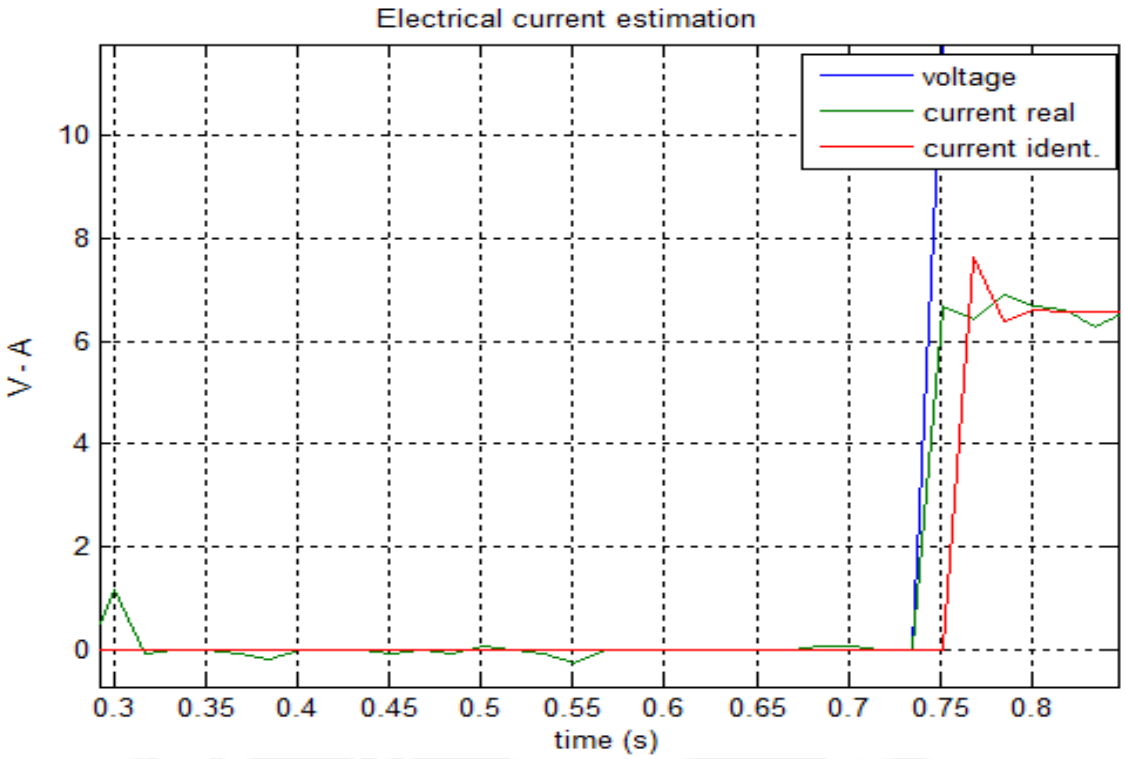

Figure 5.15: Electrical current estimation by LMS

Parameters	Value
mass (m)	1.85 kg
Electrical current stiffness coefficient k_i	-1.116 (N/A)
Displacement coefficient k_x	1.04 (N/m)
Resistance of coil R	1.89 ohm
Inductance L	1.584 H

Table 5.2: Parameters of simulation system identification by neural networking

The figure 5.22 shows the validation position with the system identifying of 3 block charts. This was simulated by *Simulink* of Matlab, the system works while the prototype is running, because with a step input signal, the position increases and when the input signal is 0, the position decreases. The figure 5.23 shows a good estimation of position according to a input signal, it has a variation minimum but is not stabilizing because not exist a controller that stabilize system, just shown the response with a input voltage signal.

Bode response of the system is shown in figure 5.24, the system work inside a large range of frequencies [0-100]Hz.

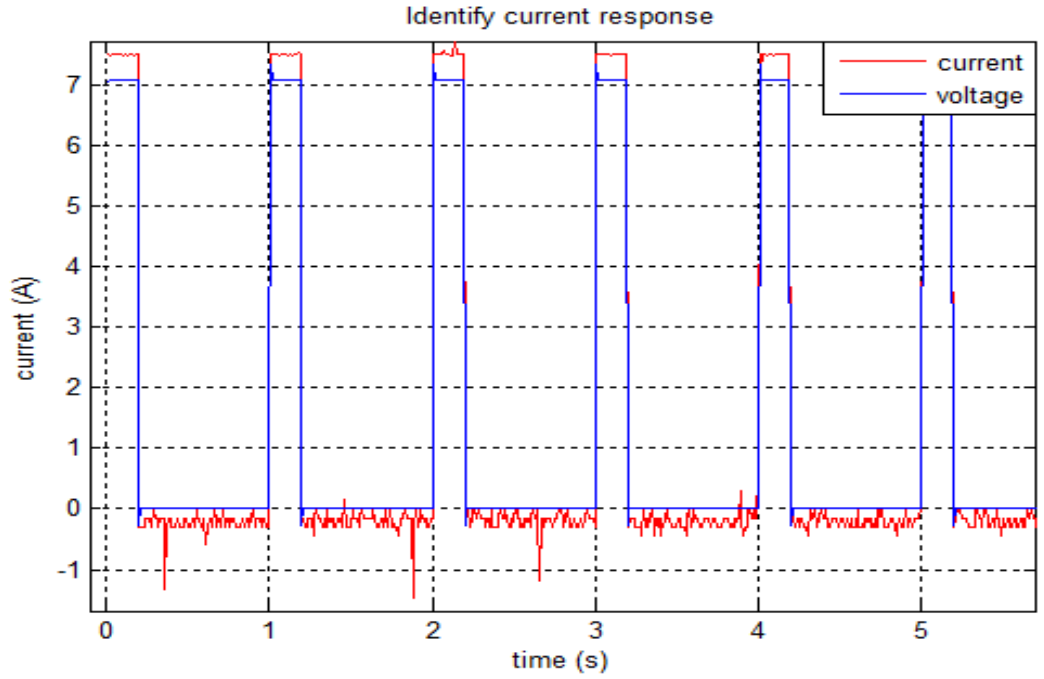

Figure 5.16: Scale values of current and voltage

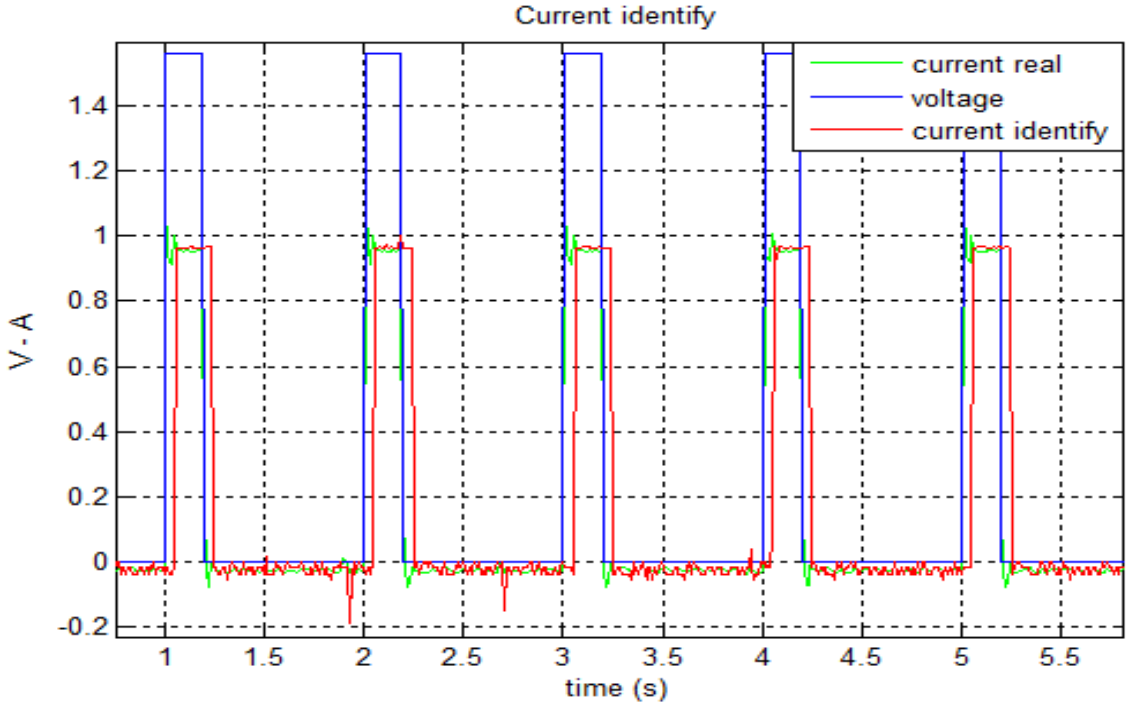

Figure 5.17: Estimate current off-line by Neural Network

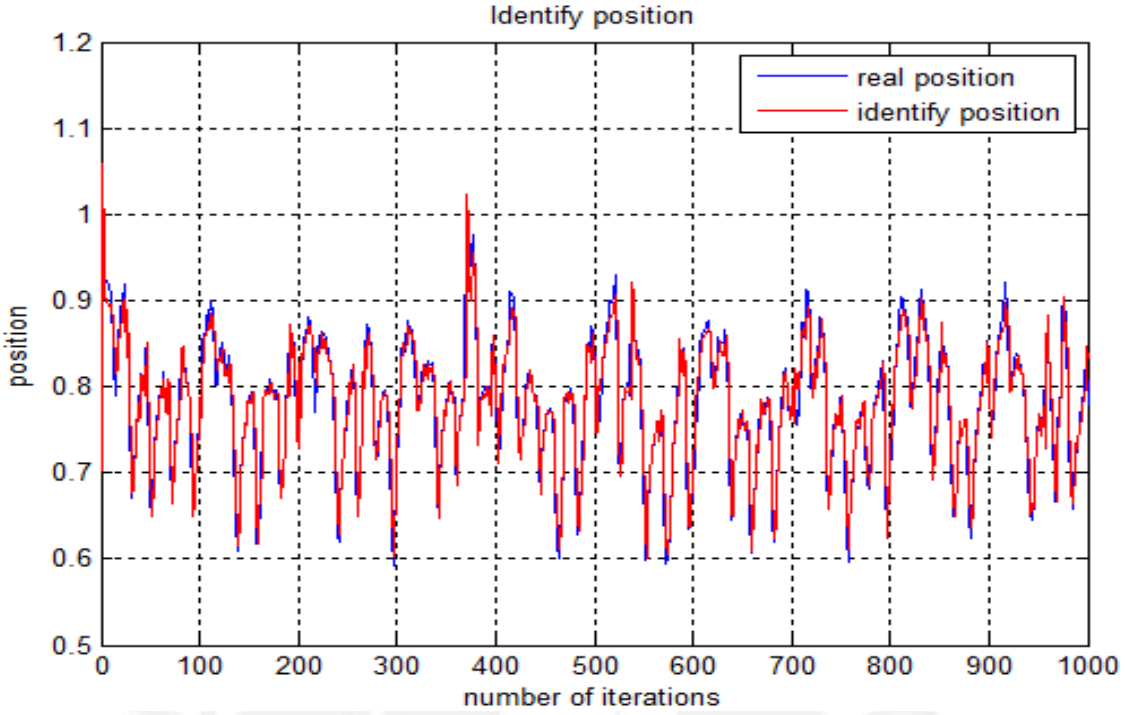

Figure 5.18: Estimate position off-line by Neural Network

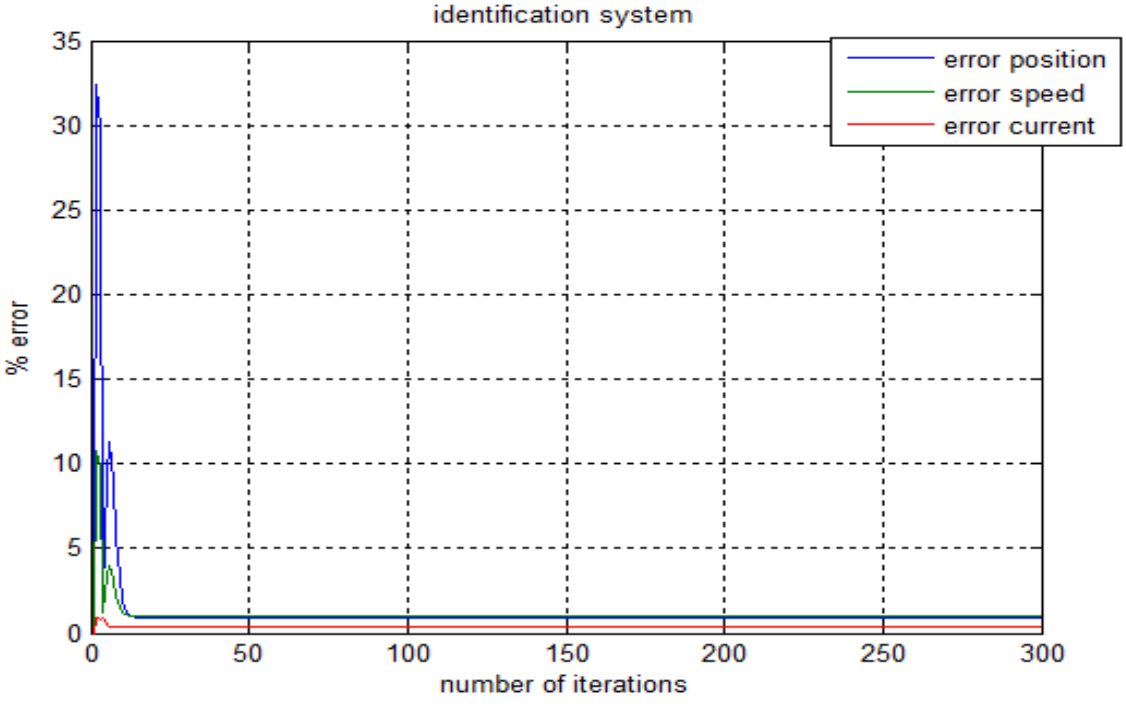

Figure 5.19: Minimization error of identifying current by Neural Network

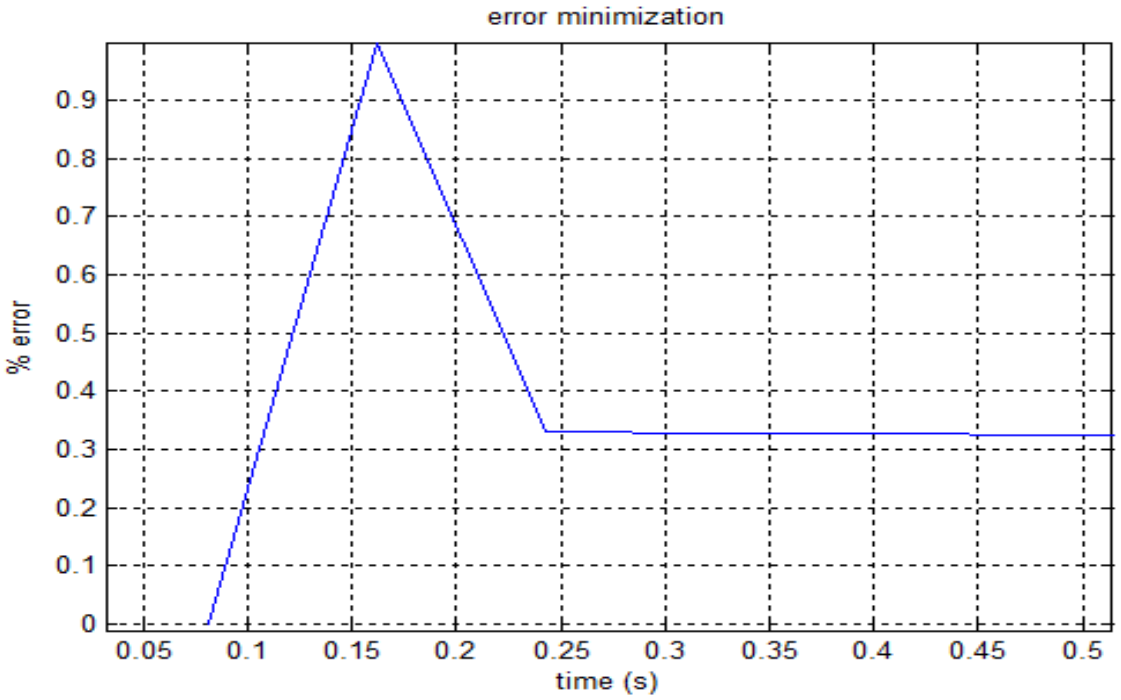

Figure 5.20: Minimization total error of identifying current by Neural Network

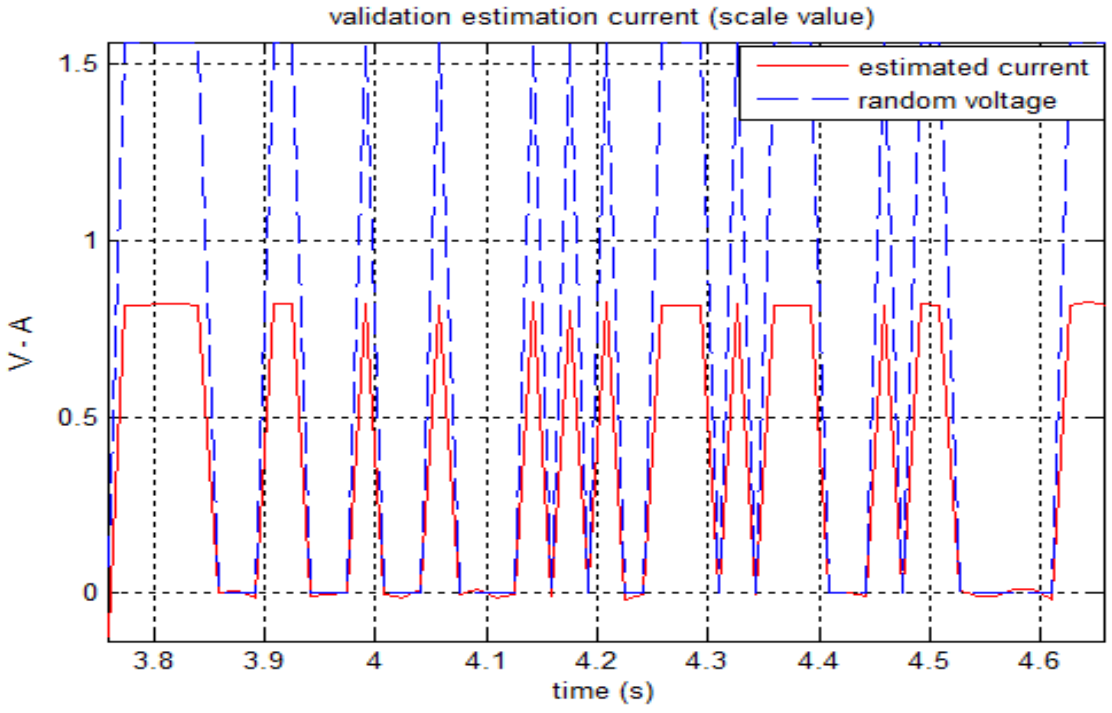

Figure 5.21: Validate of current estimation

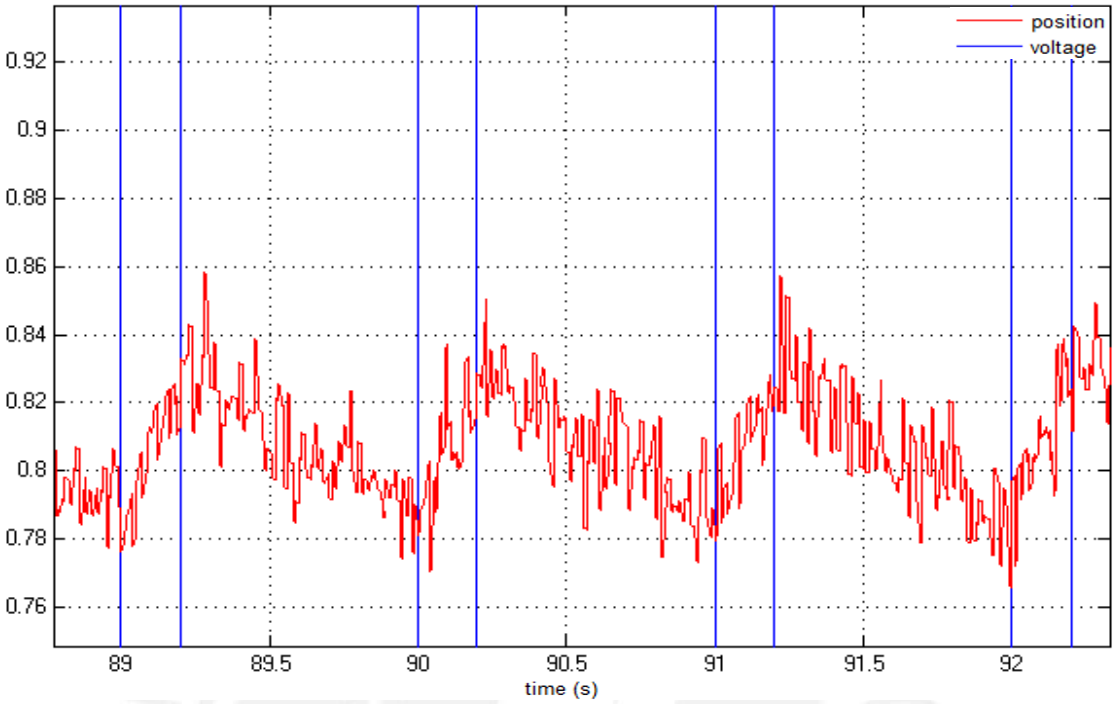

Figure 5.22: Validate of position estimation by block charts

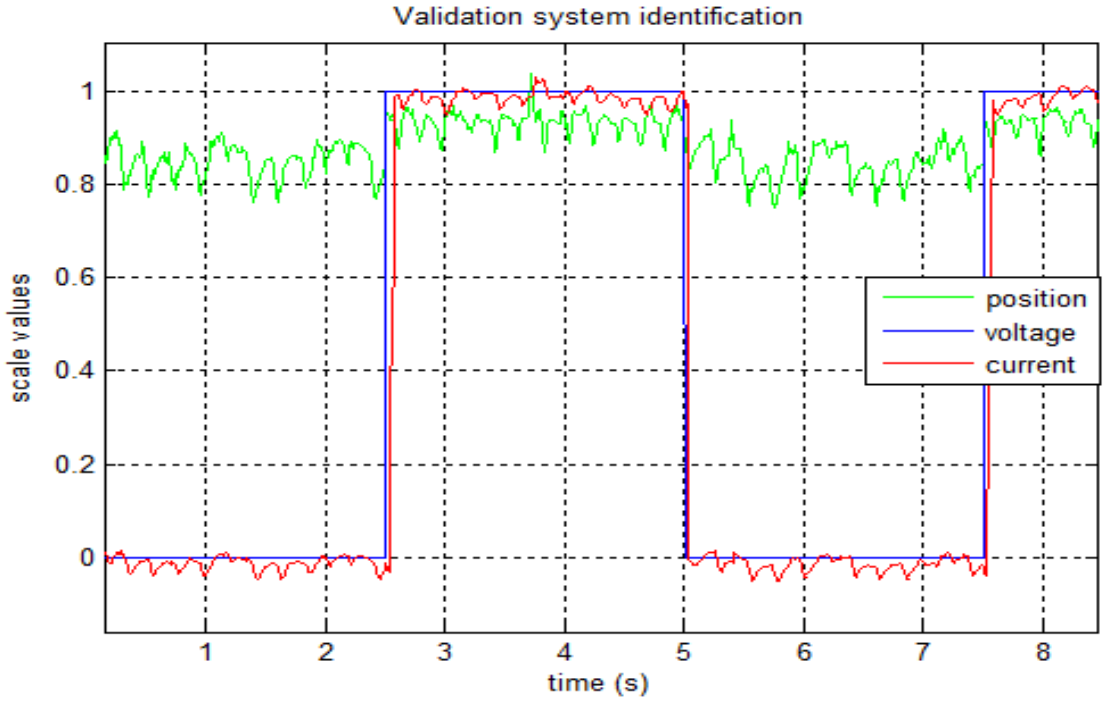

Figure 5.23: Validate of position estimation by neural networking

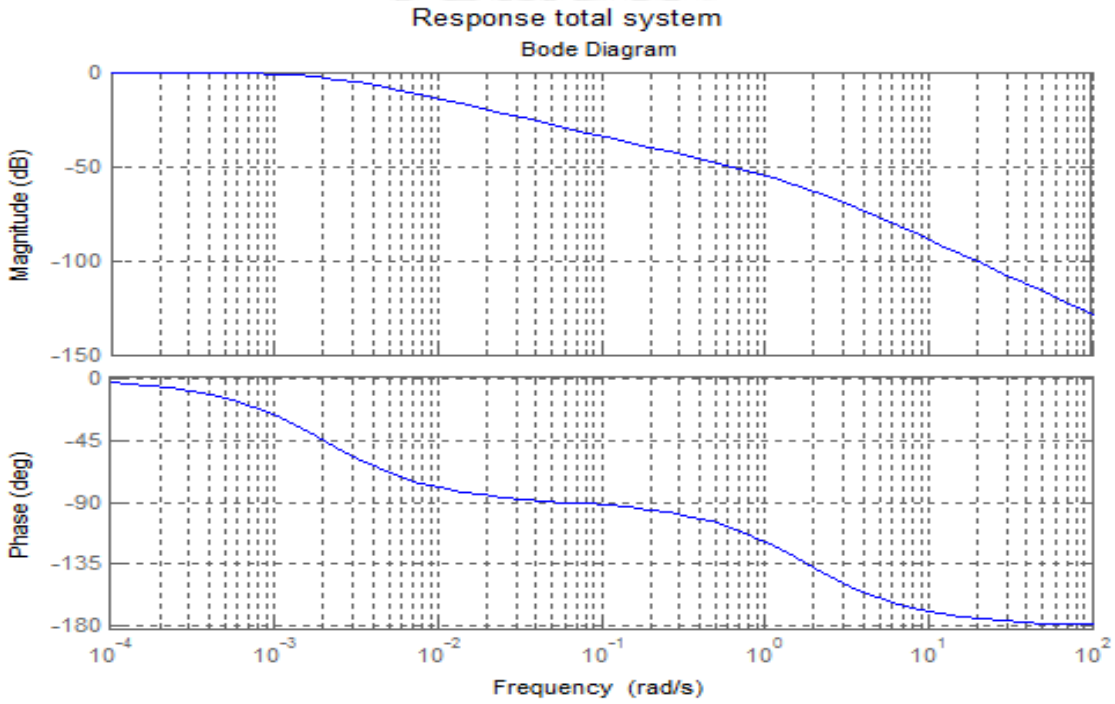

Figure 5.24: Bode response system

Chapter 6

Future work

Future works include an industrial prototype, top sensors, and better controller to verify this assumptions, because the prototype was developed with a limitation, money and access a market with the best tecnologicall components.
Also it's knowing important how works a motor to design an correct AMB prototype, the motor just transmit torque forces and radial impulse, for that, a correct mounting include two bearings and a central mass between of them.
So this bearings support are acting with transversal forces such as weight, inertia, disturbances in different axial directions. This design must considerate one of these bearings near rotor of the motor and the own motor must have a robust support.
The figure 6.1 include an idea of design a good system of AMB, but it must be developed in a completely electro-mechanical work, it would comprise a better work thesis in pre-grade program, including electro-magnetic and mechanical fields and a good understanding of physic principles.

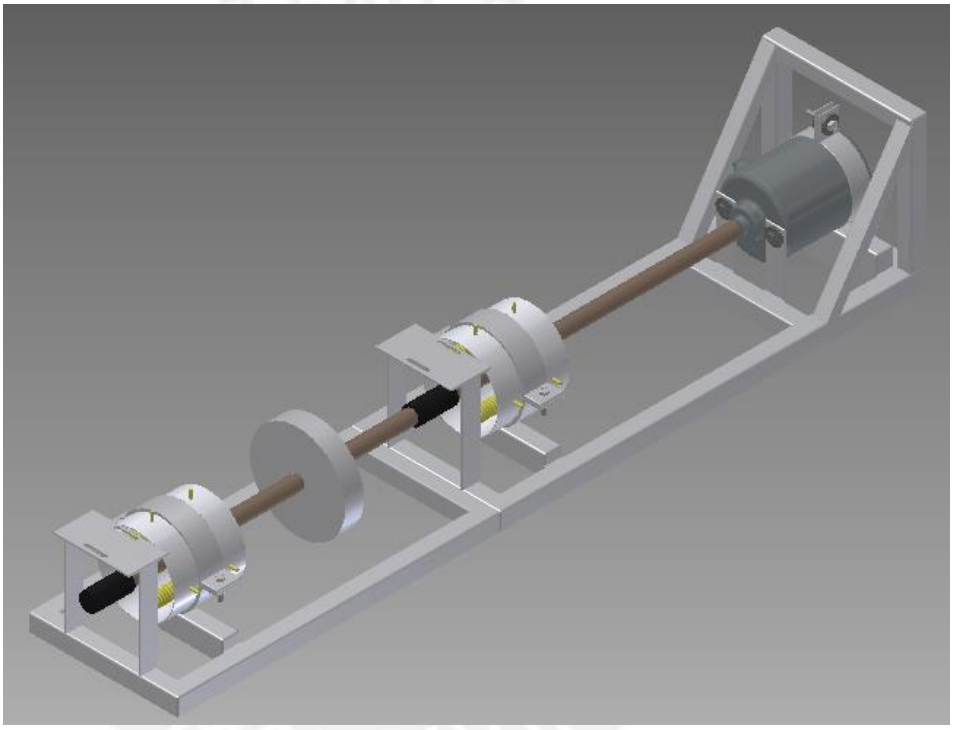

Figure 6.1: Future proposal equipment

Conclusions

Conclusions

This thesis introduced a simple structure of active magnetic bearing, in a vertical position with out gravity forces.
This model allow identify mechanical and electrical parameters to give an idea to identify industrial equipments.
The time to identify first parameters is around 5 seconds including shaping data and error minimization using neural networking.
Then time to identify and just update parameters is around 1.6 seconds and its possible include this identification inside the control system, activating with interrupter flags, working in parallel.
This prototype works as a experimental model, mechanical construction is simple and lacks with a central mass.
The error of identifying parameters with neural networking and transfer functions is around 3%, is a good estimation of response.

Bibliography

[Bar] Barcelona (1980), *Barcelona: CEAC, "Elementos de máquinas".*

[Jin] Jinji, Sun and Dong Chen (2013), *Stiffness Measurement Method of Repulsive Passive Magnetic Bearing in SGMSCMG.*

[Young] YOUNG Man Cho. (2007), *Modelling and system identification of active magnetic bearing system.*

[Noshad] A.NOSHAD. (2014), *Genetic Algorith.based System Identification of active Magnetic Bearing System: A frecuency-domain Approach.*

[Shilei] SHILEI Xu., Gan, W. and Kuo, S. (2014), *A novel Conicla Active Magnetic Bearing With Claw Structure.*

[Childs] Childs, D. (1994), *Turbomachinery Rotordynamics.* New York: Wiley.

[Lee-Yoon] Lee, C.W., Yoon, Y.K. and Jeong, H.S. (1997), *Compensation of tool axis misalignment in AMB spindle system.* KSME International Journal, 11.

[Colby] Colby, R.S. and Piech, Z.J. (1994), *Magnetic bearing: design and static test results.* United Technologies Research Center Report No. R94-170120-1.

[Mohd] Mohd-Mokhtar, L. Wang., (2004), *Continus Time System Identification of Magnetic Bearing System Using Frecuency Response Data.* 5th Asian control conference.

[Melbourne] Melbourne, Kuo, K. and Gan, W. (2010), Magnetic Bearing: Investigation on New Design and Control Methodology. RMIT University.

[Haver] B.R.J. Haverkamp, M. Verhaegen, C.T. Chou and R. Johansson. (1997), *Continuaus-time Subspace Model us- ing Laguerre Filtering.* 11th IFAC/IFORS Symp. on Identification and System Parameter Estimation, pp .1143-1148,1997.

[Ljung] Lennart Ljung.(1987), *System Identification- Theory for the user.* IEEE Transactions on Audio, Speech, and Language Processing, Vol 15, No 2.

[Jeong] C. W. Lee and H. S. Jeong. (1996), *Dynamic modeling and optimal control of cone-shaped active magnetic bearing systems.* Eng. Pract., vol. 4, no. 10, pp. 1393–1403.

[Rodriguez] Rodriguez Daniel, Alamo Teodoro. (2003), *Intorducción a la identificación de sistemas.*

[Box] Box, George; Jenkins, Gwilym.(2000), *Time Series Analysis: Forecasting and Control.* San Francisco: Holden-Day.

[Arafet] Arafet Padilla, Pedro.(2008), *Métodos de Identificación dinámica.* Facultad de Ingeniería Eléctrica Universidad de Oriente

[Rajiv] Rajiv Tiwari, Avinash Choungale. (2014), *Identification of bearing dynamic parameters and undbalance states in a flexible rotor system fully levitated on active magnetic bearing.* 8th International Symposium on Image and Signal Processing and Analysis (ISPA 2013).

[Gibson] Gibson Nathan S.(2003), *Control of active magnetic bearings using artificial neural network identification of uncertainty.* IEEE Transactions on Audio, Speech, and Language Processing, Vol. 19, No. 4.

[Ki-Chang] Ki-Chang-Lee.(2006), *Development of a radial active magnetic bearing for high speed turbo-machinery motors.* Korea.

[Calderón] Calderón, Alan. (2016), *Control Strategies for a Prototype of Active Magnetic Bearing System.* Pontificia Universidad Católica del Perú

[Guwahati] Guwahati, Jagu. and Kajikawa, Y. (2008), *Introduction to Magnetic Bearings Lecture presented in Quality Improvement Program.* Indian Institute of Technology.

[Sedano] Javier Sedano, Franco.(2013), *Representación de un sistema no lineal usando redes neuronales.* Area de Tecnología Electrónica de la Universidad de Burgos.

[Heeju] Heeju Choi Gregory D. Buckner.(2012), *H, Control of Active Magnetic Bearings Using Artificial Neural Network Identification of Uncertainty.*

[Gerhard] Gerhard Schweitzer, Eric H Maslen .(2009), *Magnetic Bearings, Theory, Design, and Application to rotatory machinery.* Springer

APPENDIX

A. Mechanical drawing

B. Electrical drawing

C. Paper